Vibration Signals Analysis by Explainable Artificial Intelligence (XAI) Approach

Ching-Hung Lee

Department of Electrical and Computer Engineering
National Yang Ming Chiao Tung University
Taiwan

ICALAB
智慧型控制及應用實驗室

Ching-Hung Lee
(李慶鴻)
Professor

Office: EE761
E-mail：chl@nycu.edu.tw
ICA Lab. EE606

Education Profile：

- **Ph.D.**, Electrical and Control Engineering, National Chiao Tung University, Taiwan
- **M.S.**, Control Engineering, National Chiao Tung University, Taiwan
- **B.S.**, Control Engineering, National Chiao Tung University, Taiwan

Professional Profile：

- **Professor (2020 – present),** Institute of Electrical and Computer Engineering, National Yang Ming Chiao Tung University, TW
- **Distinguished Professor (2018 – 2020),** Dept. of ME, National Chung Hsing University, TW
- **Professor (2014 – 2018),** Dept. of ME, National Chung Hsing University, TW

Research Interests：

- Intelligent Systems Design
- Control of Robot Manipulator and Applications
- Artificial Intelligence and Applications

ICALAB
智慧型控制及應用實驗室

Artificial Intelligence

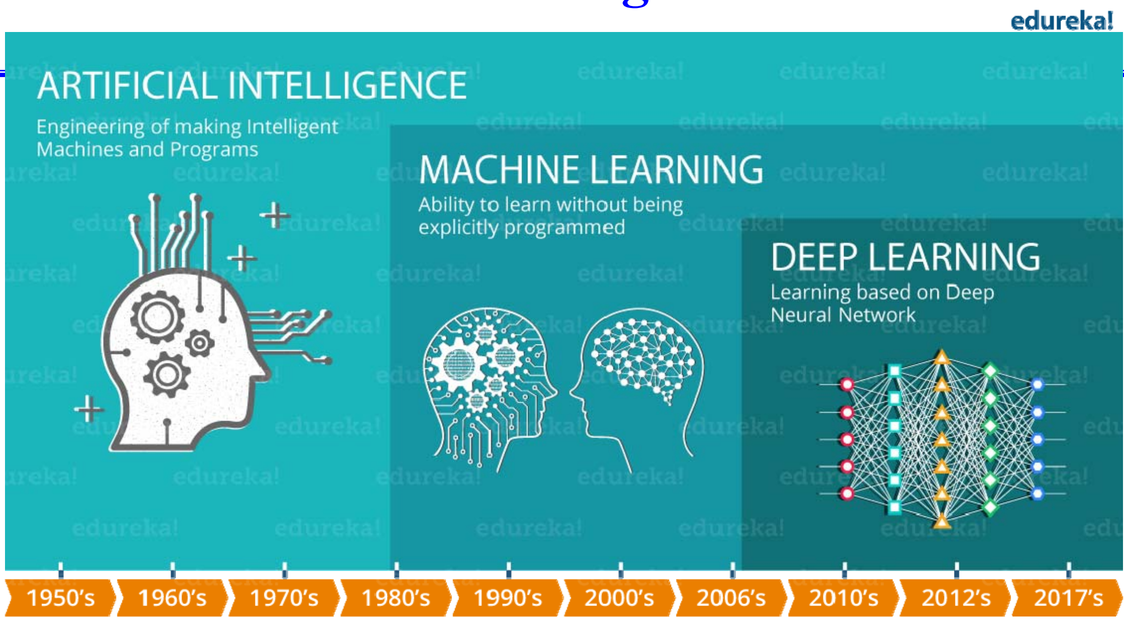

John McCarthy 1955: 人工智慧就是要讓機器的行為看起來就像是人表現出智慧的行為一樣。

AI Methodology and Applications

- 自然語言處理 (Natural language processing)
- 智慧搜索 (AI search)
- 圖形識別 (Pattern Recognition ; 樣式識別)
- 機器學習 (Machine Learning)
- 知識庫系統(Knowledge-based systems)
- 推理 (Reasoning)
- 邏輯程式設計 (Logic programming)
- 專家系統 (Expert system)
- 類神經網路 (Neural network)
- 基因演算法(Genetic algorithm)
- 模糊理論 (Fuzzy theory)
- 大數據(Big Data)….

NN Structure
卷積類神經網路(convolutional neural network)
深度神經網路(Deep neural network)
遞迴式神經網路(recurrent neural network)
自動編碼器(Autoencoder)
生成對抗網路(Generative Adversarial Network)
長短記憶體網路(Long Short Time Memory)

Learning
增強式學習(Reinforcement learning, RL)
轉移學習(transfer learning)…

I Know Machine Learning

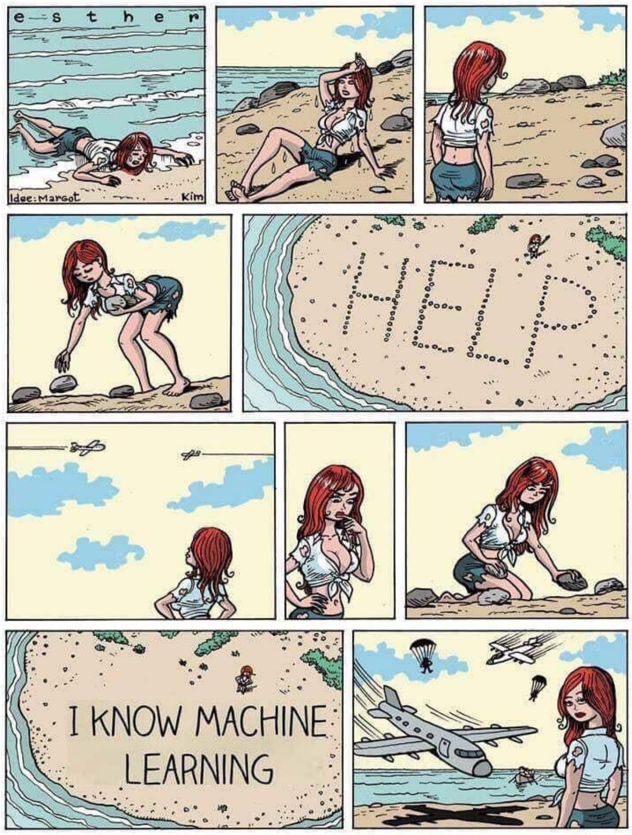

Which face is real?

http://www.whichfaceisreal.com/index.php

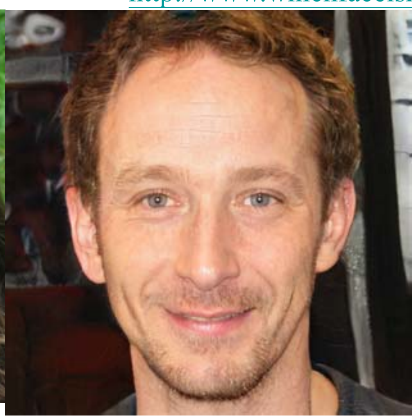

影像應用&生成

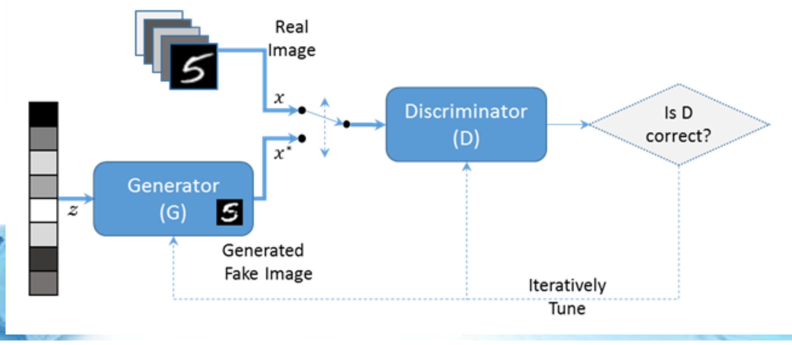

Deep Learning

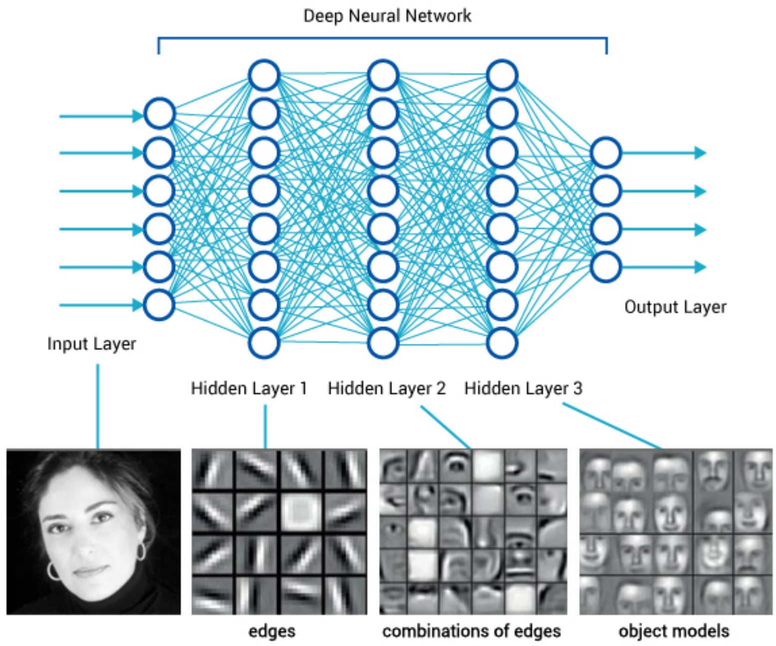

Deep learning for Classfication

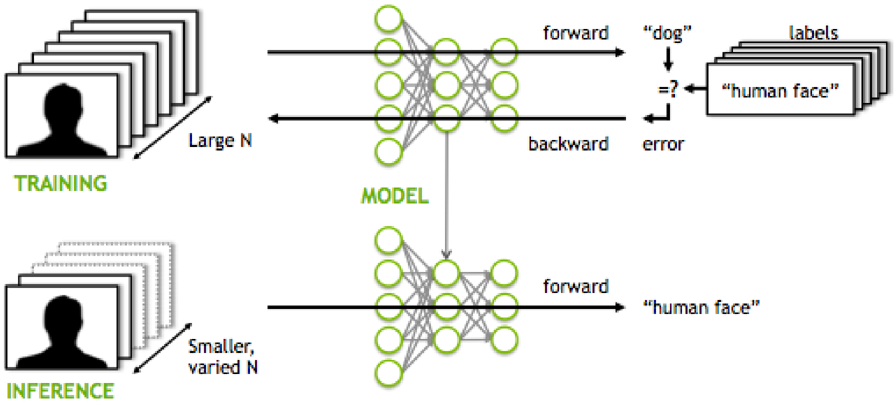

How to use AI for Smart Machinery (Manufacturing)?

Categories of AI using Neural Networks

- Data is ready
  - Problem is prediction
- Data is ready
  - Problem is classification

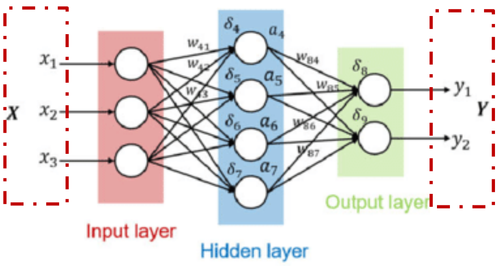

(a)

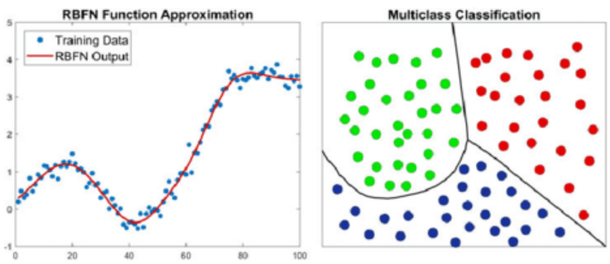

(b)

prediction

classification

Key point:
select proper input/output variables

Categories of AI using Neural Networks

- Data should be collected
  - ➢ Using Domain knowledge (physical meaning) to select proper variables
  - ➢ Experiment Design
    - Random values
    - Taguchi method
    - Uniform Experimental Design (UED)
  - ➢ Data Collection
  - ➢ Data processing and analysis
    - Correlation analysis
    - Data clearing
  - ➢ Neural network training

AI for Vibration Signals Analysis vs. Machine Diagnosis

故障診斷vs. 信號分析

Rolling Element Bearings

- **Bearings are highly engineered, precision-made components that enable machinery to move at extremely high speeds and carry remarkable loads with ease and efficiency.**
- **Bearings are found in applications ranging from small hand-held devices to heavy duty industrial systems.**

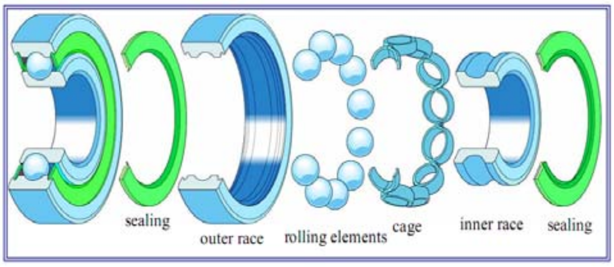

故障診斷vs. 信號分析

Bearing Defects

Localized defects

i) Cracks
ii) Pits
iii) Spalls

Cause : Fatigue on rolling surfaces

Distributed defects

i) Surface Waviness
ii) Misaligned races
iii) Off-size rolling elements

Cause : Manufacturing errors, ***Wear***

(a) (b)

(c)

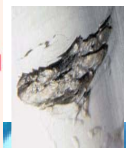

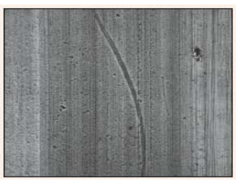

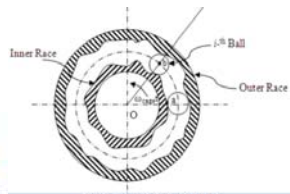

Race waviness model

故障診斷vs. 信號分析

- Localized defects in bearing elements

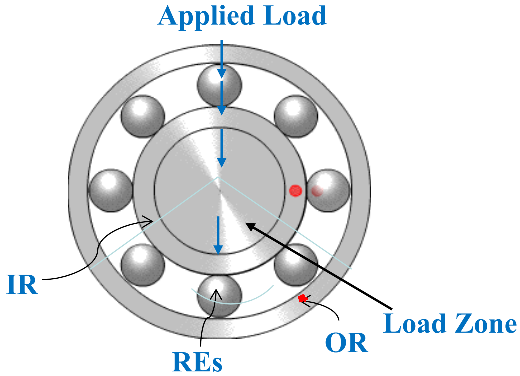

STEP:1 DATA ACQUISITION
⇩
STEP:2 FEATURE EXTRACTION USING SIGNAL PROCESSING TECHNIQUES
⇩
STEP:3 DECISION MAKING

故障診斷vs. 信號分析

Vibration Signal Processing

- **1. Time-domain approach** → Non-Stationary Signals
- **2. Freq.-domain approach** → Stationary Signals
- **3. TF domain approach** → Non-Stationary Signals, Stationary Signals

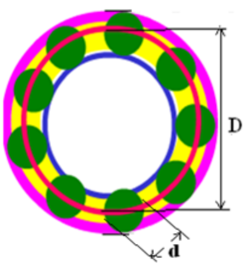

	Characteristic defect frequency	Expression
•Outer race	Outer race defect frequency, ω_{od}	$(Z\,\omega_s/2)[1-(d/D)\cos\alpha]$
•Inner race	Inner race defect frequency, ω_{id}	$(Z\,\omega_s/2)[1+(d/D)\cos\alpha]$
•Rolling element	Rolling element defect frequency, ω_{red}	$(D\,\omega_s/d)[1-(d^2/D^2)\cos^2\alpha]$
•Cage	Cage frequency, ω_c	$(\omega_s/2)[1-(d/D)\cos\alpha]$
•Lubricant		

d is the roller diameter D is pitch diameter ω_s is shaft rotational speed Z is number of balls

Modeling

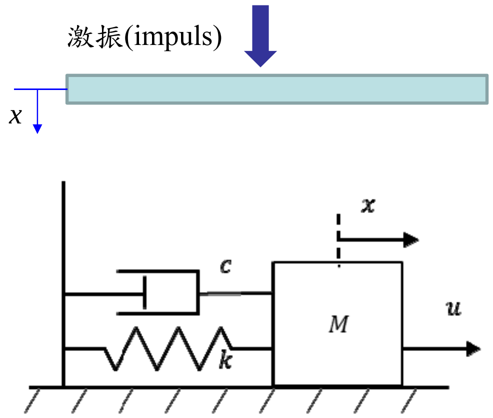

$M\ddot{x} + c\dot{x} + kx = u$

Vibratory Model of Bearing

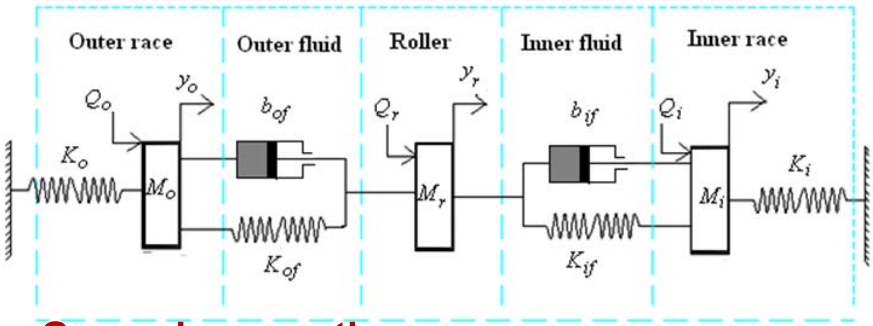

Governing equations:

$$[M]\{\ddot{y}\}+[B]\{\dot{y}\}+[K]\{y\}=\{Q\}$$

$\{Q\}$ = **Excitation vector with excitations due to defects on bearing elements**

MATLAB- Rolling Element Bearing Fault Diagnosis

https://www.mathworks.com/help/predmaint/ug/Rolling-Element-Bearing-Fault-Diagnosis.html

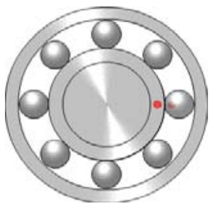

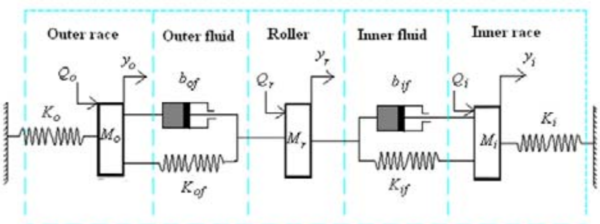

Bechhoefer, Eric. "Condition Based Maintenance Fault Database for Testing Diagnostics and Prognostic Algorithms." 2013. https://www.mfpt.org/fault-data-sets/

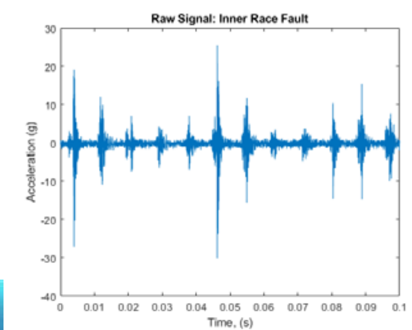

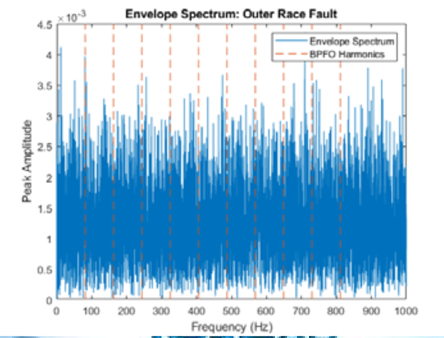

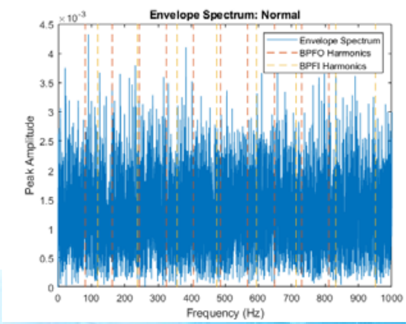

Explainable Artificial Intelligence (XAI) for Vibration Signals Analysis: Bearing Faults Classification Using CNNs

科技發展趨勢

事件影響	發生年份	項次
造紙	105	1
火藥	900	2
機械計算機	1623	3
牛頓三大定理	1687	4
蒸汽機	1760	5
基因工程	1865	6
狹義相對論	1905	7
量子力學	1927	8
電腦	1939	9
人工智慧	1956	10
網路	1974	11
智慧型手機	1992	12
人類基因排序	2006	13
大數據	2009	14
物聯網	2010	15
量子通訊	2017	16
量子電腦	2019	17
5G	2020	18
元宇宙	2021	19

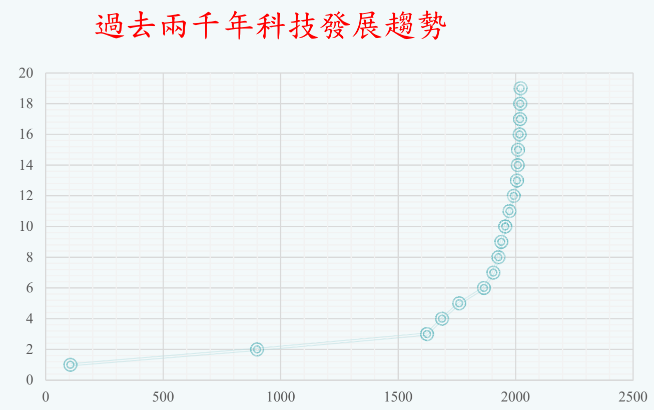

Deep Learning vs. Machine Learning

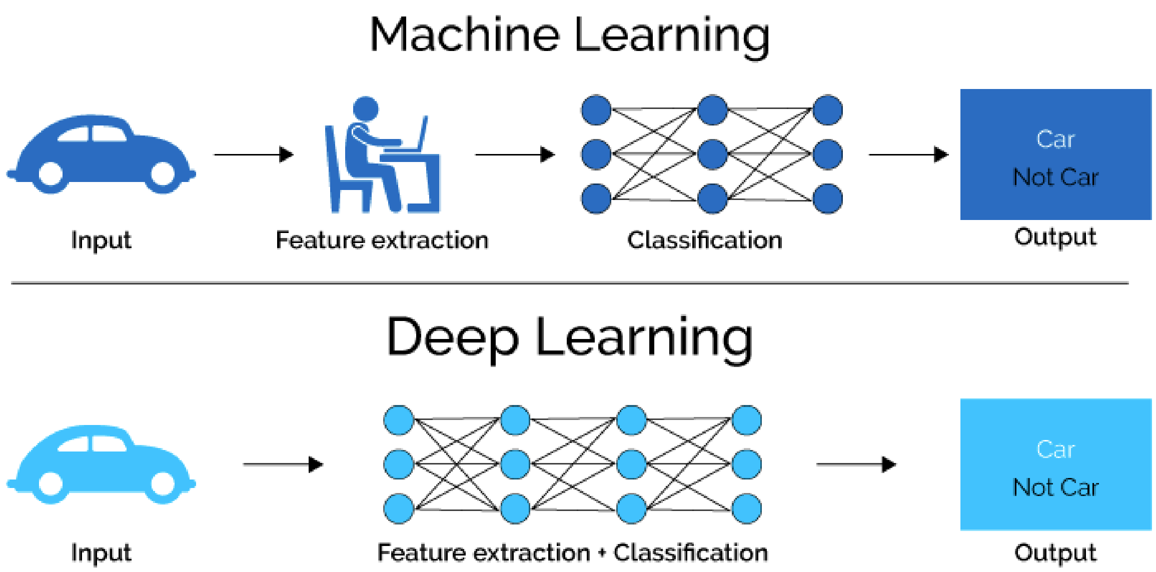

Why Explainable Artificial Intelligence?

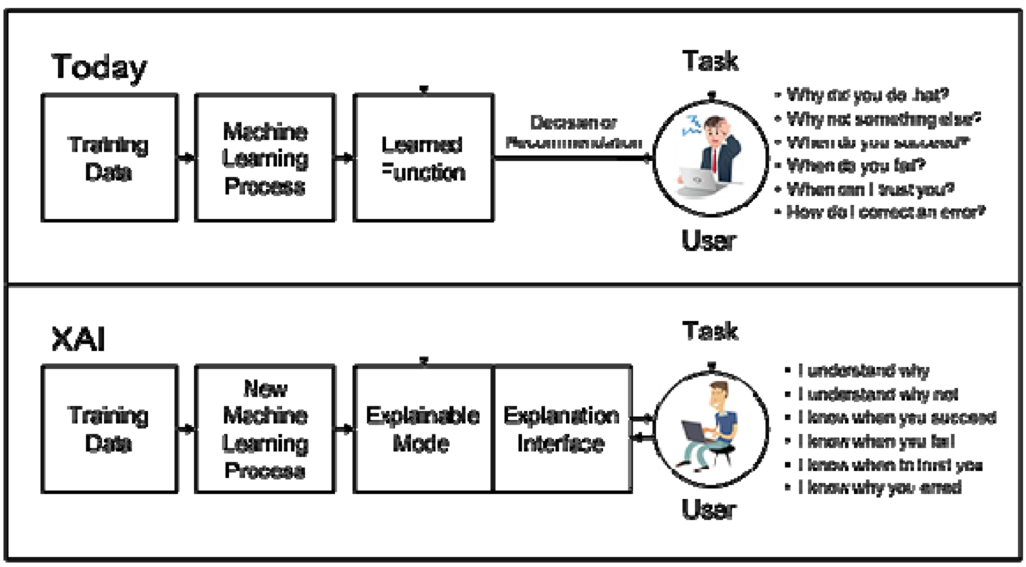

http://groupementadas.canalblog.com/archives/2018/08/23/36639574.html

Why Explainable Artificial Intelligence?

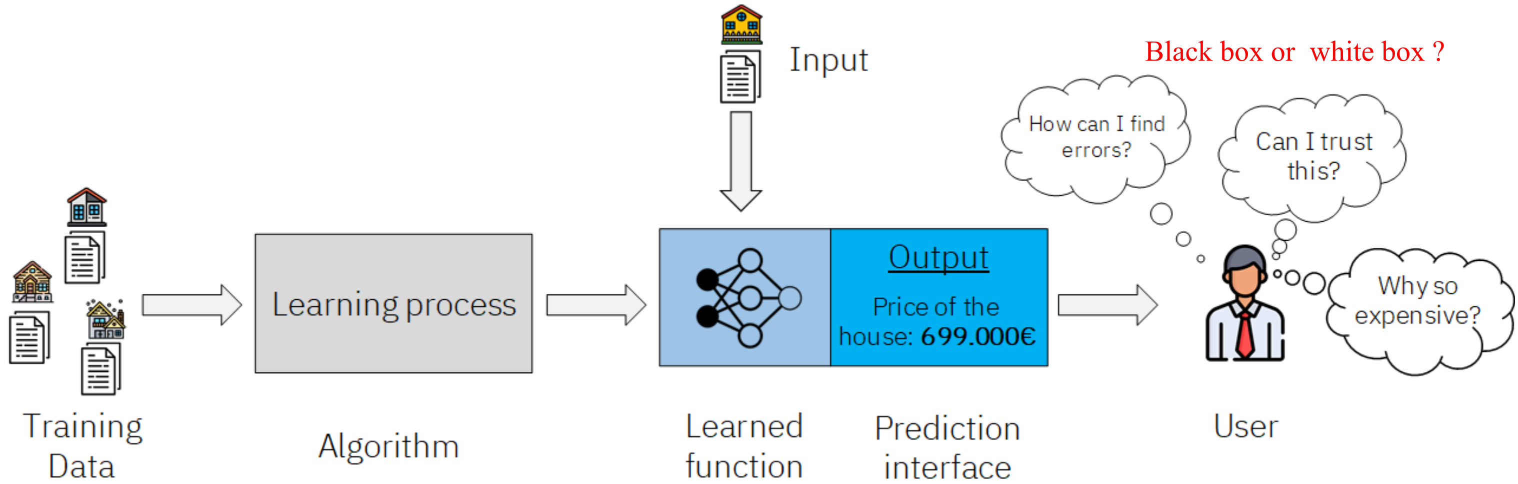

https://towardsdatascience.com/explainable-artificial-intelligence-14944563cc79

Why Explainable Artificial Intelligence?

Evolutionary Fuzzy Systems

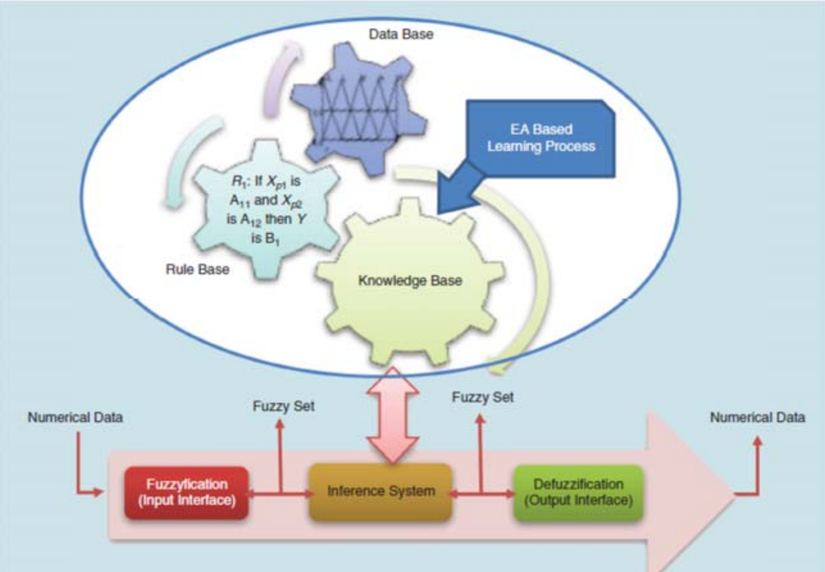

https://ieeexplore.ieee.org/stamp/stamp.jsp?tp=&arnumber=8610271

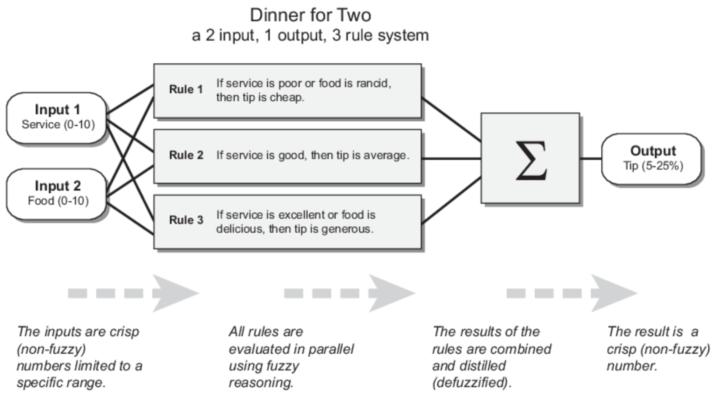

https://es.mathworks.com/help/fuzzy/fuzzy-inference-process.html

Evolutionary Fuzzy Systems vs. XAI

https://link.springer.com/chapter/10.1007/978-3-030-04070-3_1

Rolling Element Bearing Fault Diagnosis

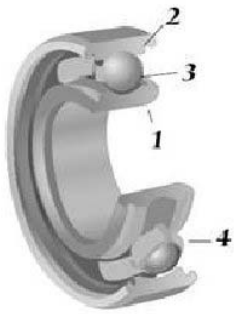

1. Inner Race
2. Outer Race
3. Balls
4. Cage

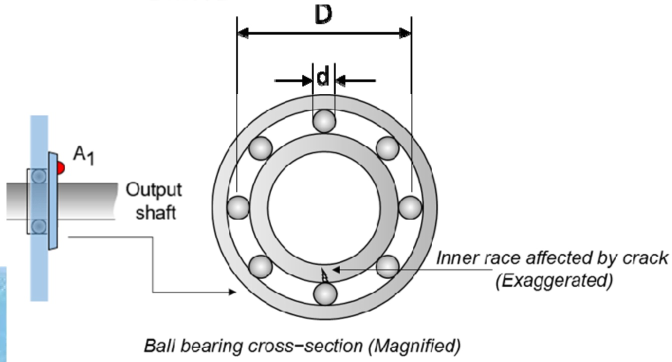

$$BPFO = \frac{nf_r}{2}(1-\frac{d}{D}\cos\phi)$$

$$BPFI = \frac{nf_r}{2}(1+\frac{d}{D}\cos\phi)$$

$$FTF = \frac{f_r}{2}(1-\frac{d}{D}\cos\phi)$$

$$BSF = \frac{D}{2d}(1-(\frac{d}{D}\cos\phi)^2)$$

https://www.mathworks.com/help/predmaint/ug/Rolling-Element-Bearing-Fault-Diagnosis.html

Rolling Element Bearing Fault Diagnosis

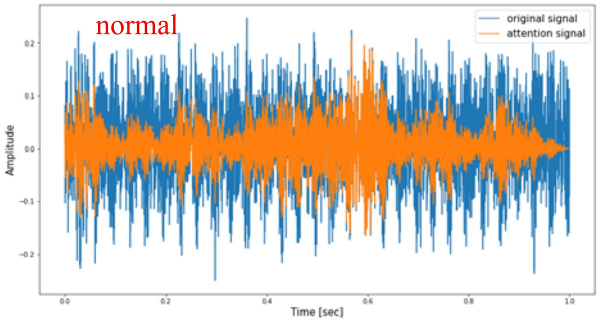

Features?

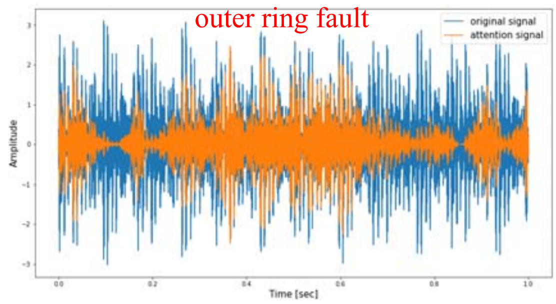

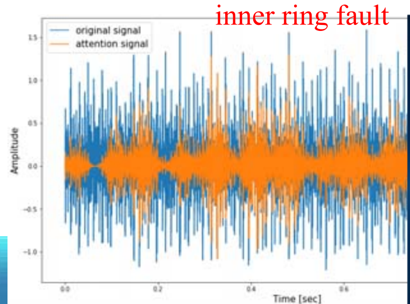

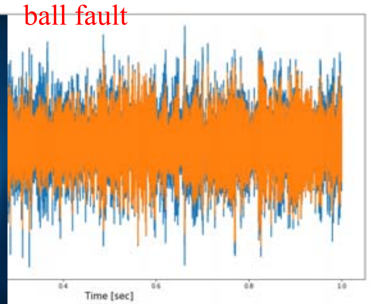

Bear Fault Diagnosis and Monitoring

- 分析機台振動信號進行關鍵零組件診斷
- 使用 NASA 及 PHM 的開放式資料庫預測軸承壽命
  - 建立深度學習模型進行「即時」診斷
  - 導入 *Transfer Learning*，以降低大量訓練資料的需求

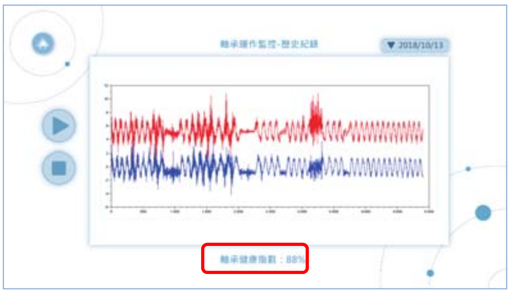

透過LINE robot or App
即時通知使用者

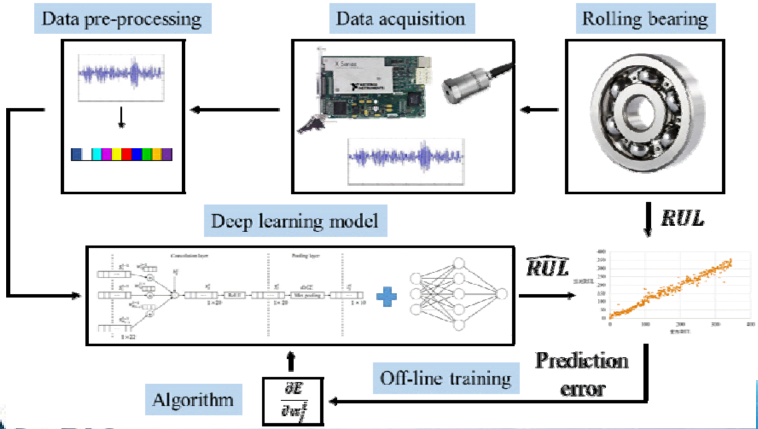

機台關鍵零組件-軸承運作監控與診斷

- Center on Intelligent Maintenance Systems (IMS)
- IEEE PHM 2012 Prognostic challenge

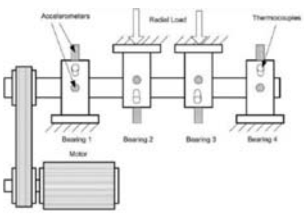

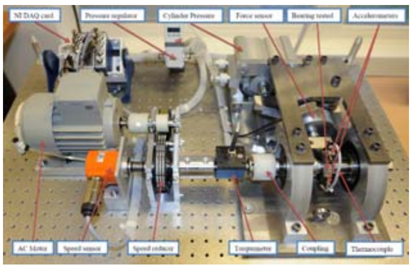

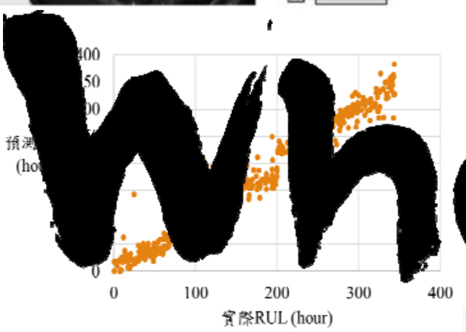

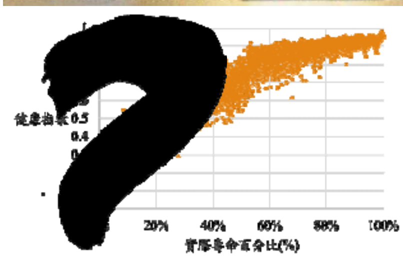

則結果與實際比較

Brief Introduction for Powerful Artificial Neural Network- *Convolutional Neural Network*

ICALab
智慧型控制及應用實驗室

Convolutional Neural Networks

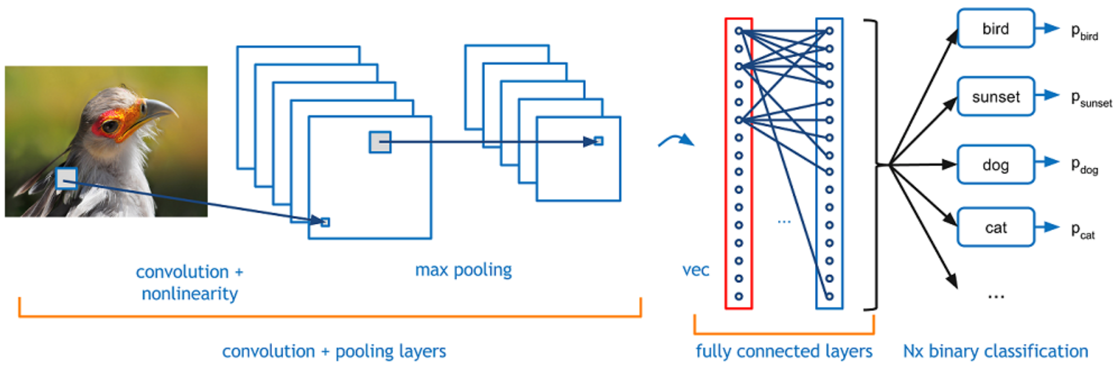

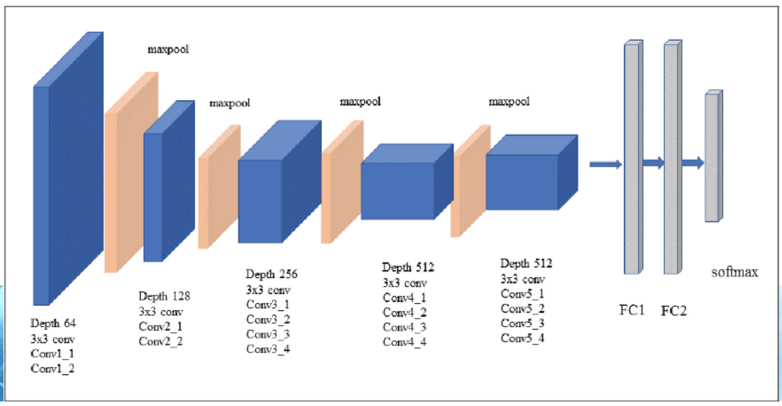

VGG19

Consider learning an image:

- Some patterns are much smaller than the whole image

Can represent a small region with fewer parameters

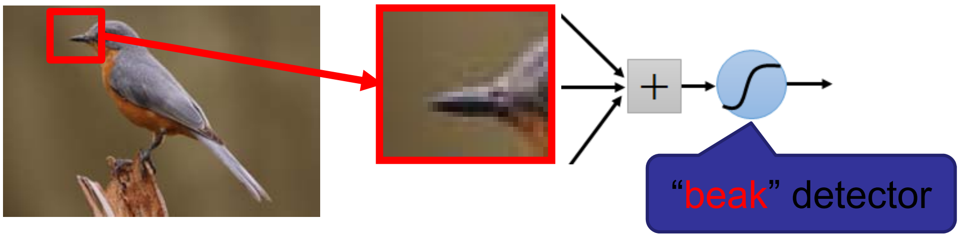

Same pattern appears in different places: They can be compressed! What about training a lot of such "small" detectors and each detector must "move around".

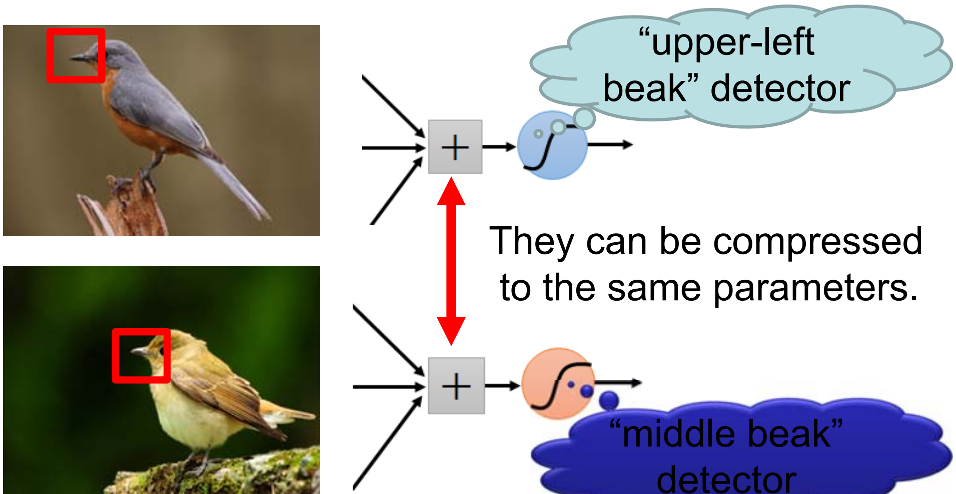

ICALAB
智慧型控制及應用實驗室

A convolutional layer

A CNN is a neural network with some convolutional layers (and some other layers). A convolutional layer has a number of filters that does convolutional operation.

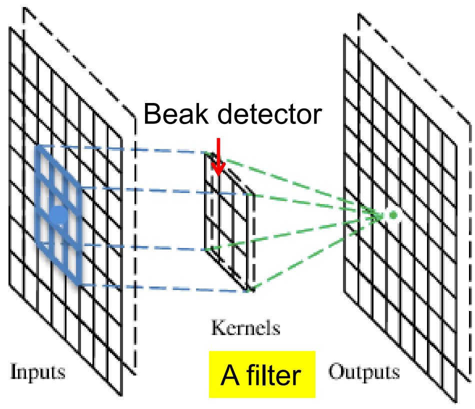

Convolution

These are the network parameters to be learned.

1	0	0	0	0	1
0	1	0	0	1	0
0	0	1	1	0	0
1	0	0	0	1	0
0	1	0	0	1	0
0	0	1	0	1	0

6 x 6 image

Filter 1

1	-1	-1
-1	1	-1
-1	-1	1

Filter 2

-1	1	-1
-1	1	-1
-1	1	-1

⋮ ⋮

Each filter detects a small pattern (3 x 3).

Convolution

1	-1	-1
-1	1	-1
-1	-1	1

Filter 1

stride=1

1	0	0	0	0	1
0	1	0	0	1	0
0	0	1	1	0	0
1	0	0	0	1	0
0	1	0	0	1	0
0	0	1	0	1	0

Dot product → 3 -1

6 x 6 image

Convolution

1	-1	-1
-1	1	-1
-1	-1	1

Filter 1

If stride=2

1	0	0	0	0	1
0	1	0	0	1	0
0	0	1	1	0	0
1	0	0	0	1	0
0	1	0	0	1	0
0	0	1	0	1	0

3 -3

6 x 6 image

ICALAB
智慧型控制及應用實驗室

Color image: RGB 3 channels

Filter 1

1	-1	-1
-1	1	-1
-1	-1	1

Filter 2

-1	1	-1
-1	1	-1
-1	1	-1

Color image

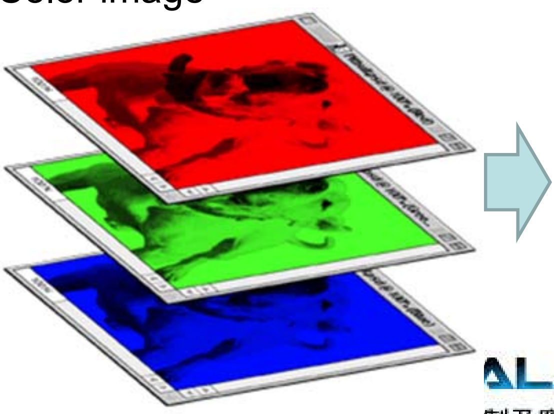

1	0	0	0	0	1
0	1	0	0	1	0
0	0	1	1	0	0
1	0	0	0	1	0
0	1	0	0	1	0
0	0	1	0	1	0

The whole C

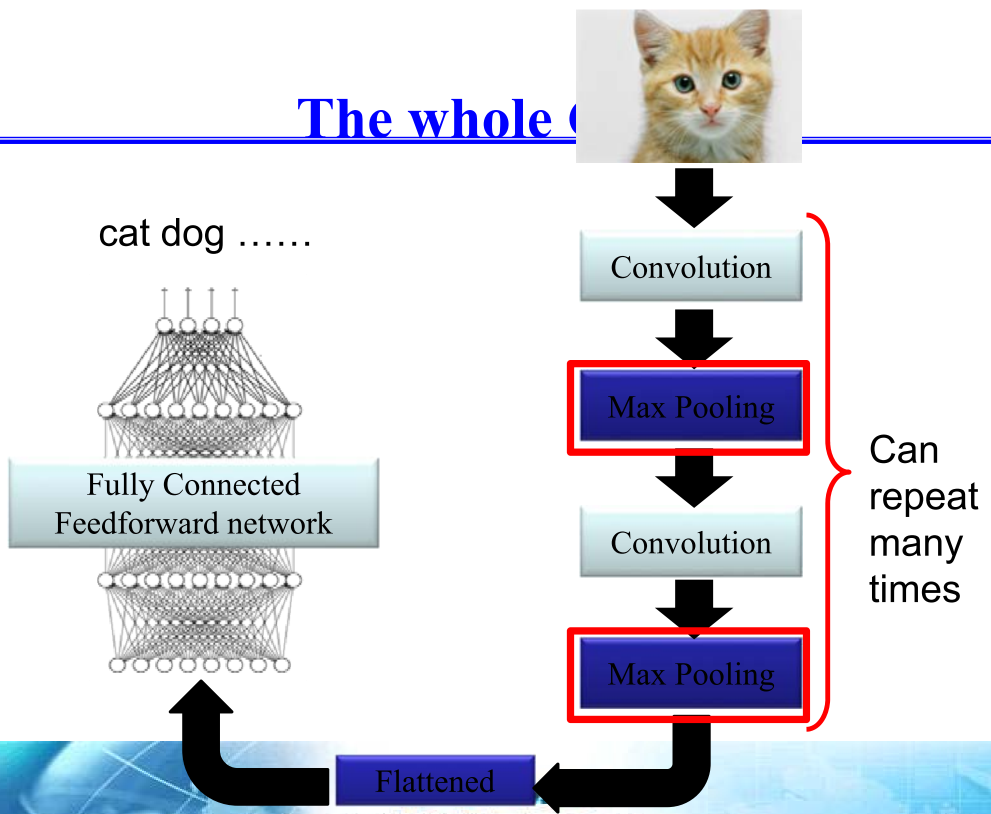

智慧型控制及應用實驗室

Max Pooling

1	-1	-1
-1	1	-1
-1	-1	1

Filter 1

-1	1	-1
-1	1	-1
-1	1	-1

Filter 2

3	-1	-3	-1
-3	1	0	-3
-3	-3	0	1
3	-2	-2	-1

-1	-1	-1	-1
-1	-1	-2	1
-1	-1	-2	1
-1	0	-4	3

Why Pooling

- Subsampling pixels will not change the object

bird

Subsampling

bird

We can subsample the pixels to make image smaller

fewer parameters to characterize the image

The whole C

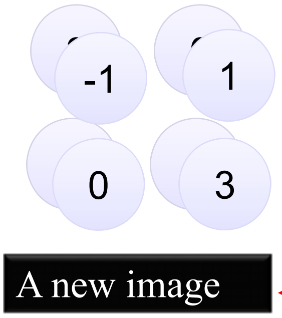

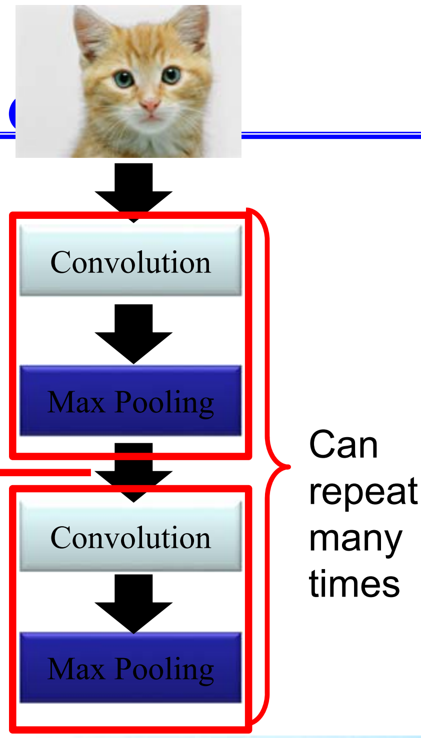

Smaller than the original image

The number of channels is the number of filters

The whole C

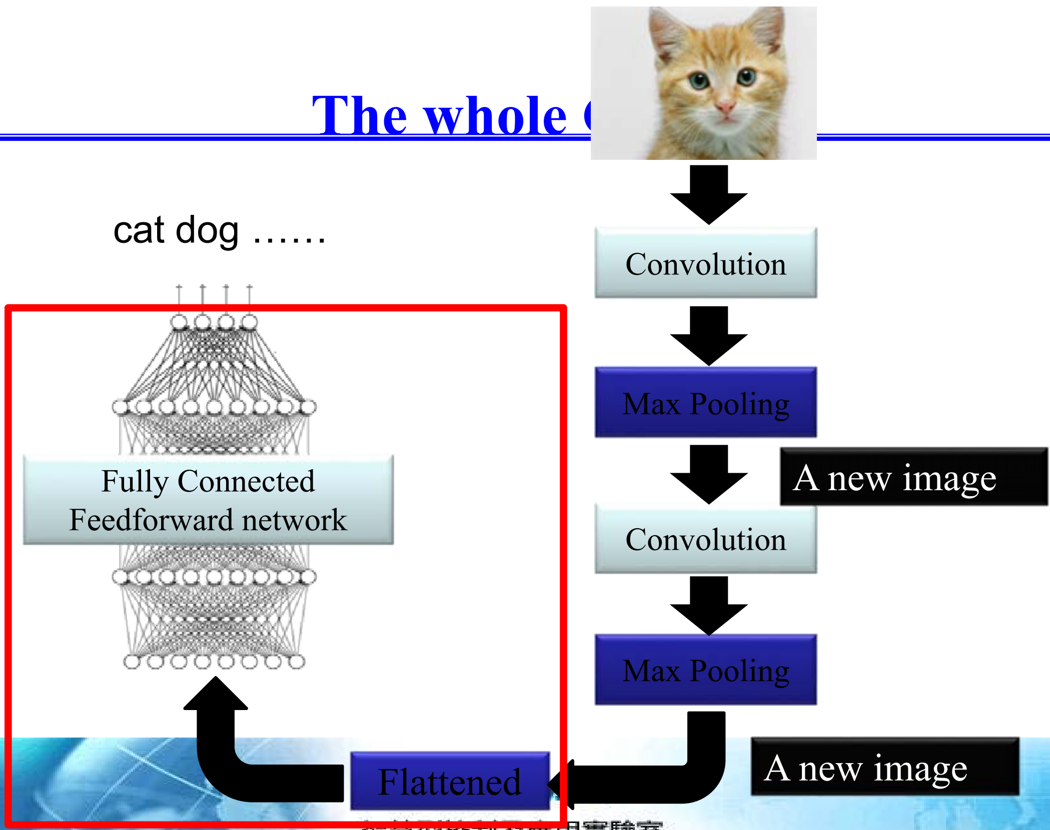

Flattening

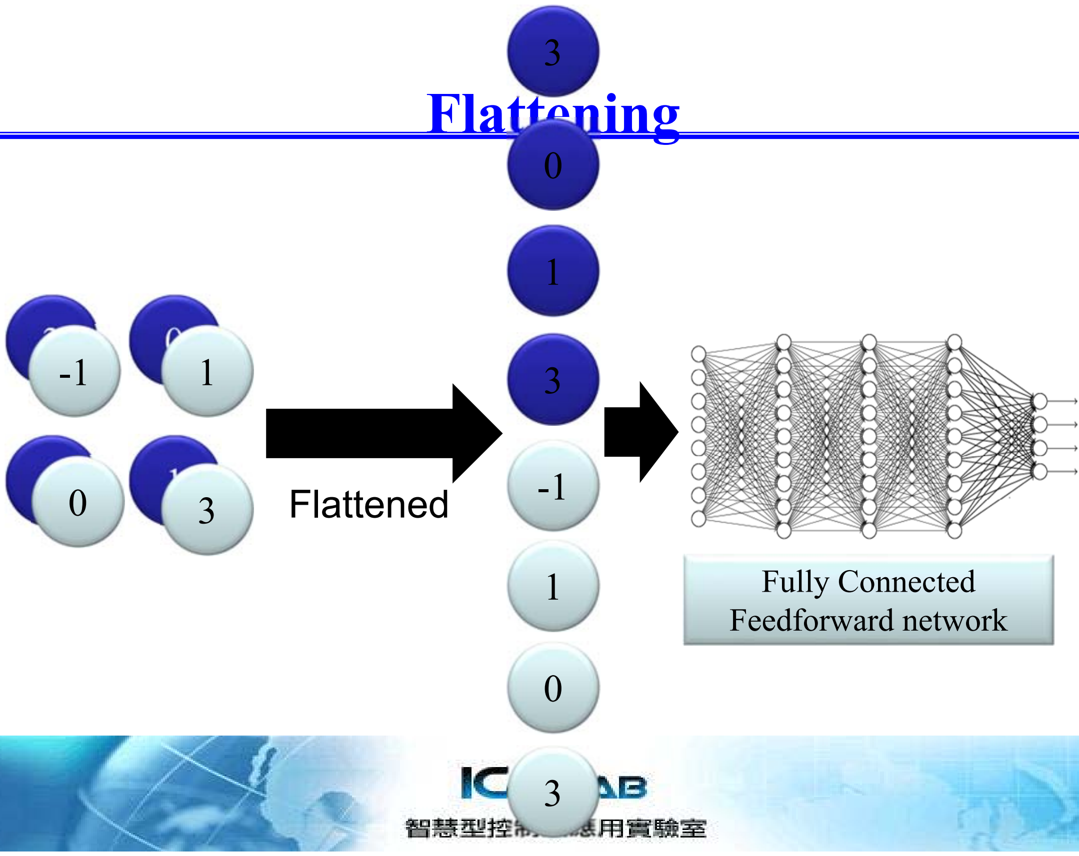

Convolutional Neural Networks

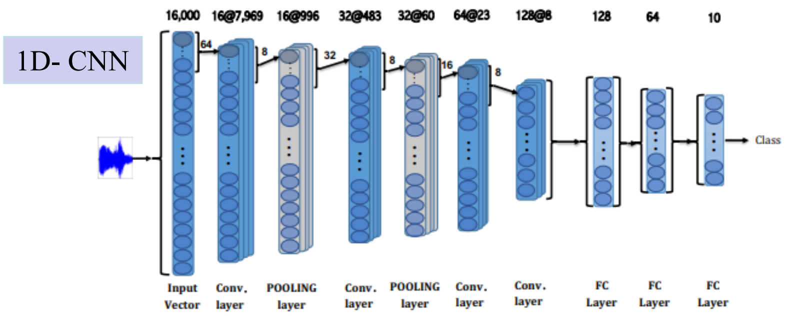

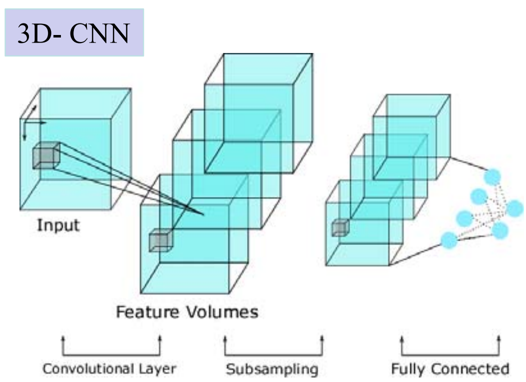

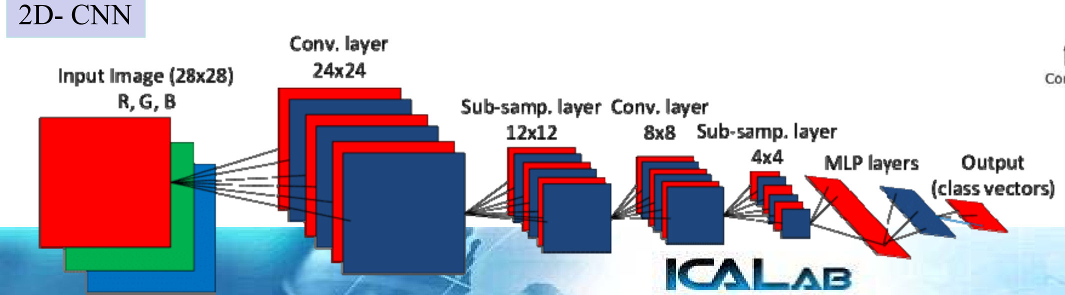

Convolutional Neural Networks (CNN)

- Proposed by Y. Lecun et al. (1998)
- Basic operations:
  - ➢ Convolutional layer
  - ➢ Pooling layer
  - ➢ Fully-connected layer
- Extract features automatically.
- 1DCNN and 2DCNN are applied as model according to different inputs.

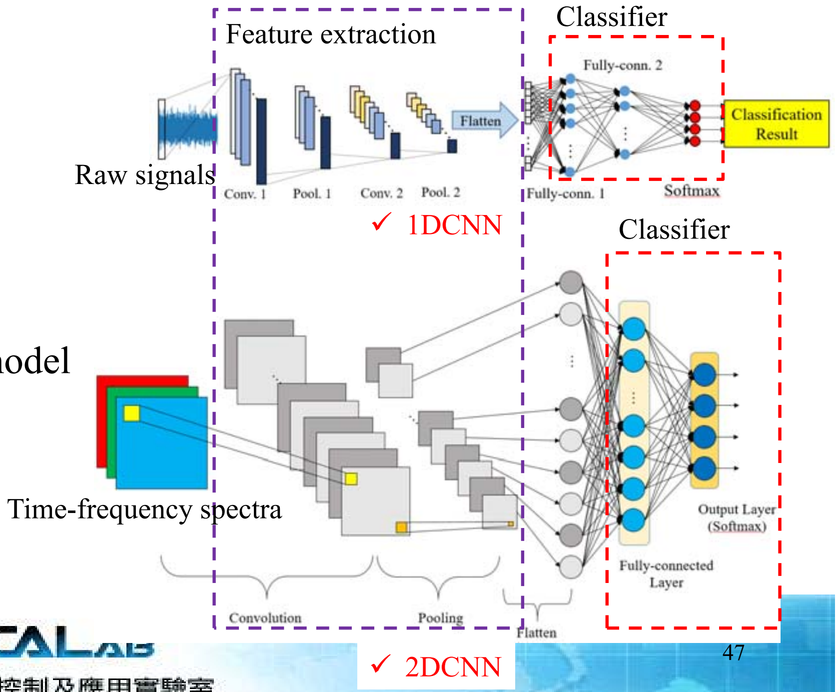

Y. Lecun, L. Bottou, Y. Bengio, and P. Haffner, "Gradient-based learning applied to document recognition," *Proceedings of the IEEE,* vol. 86, no. 11, pp. 2278-2324, 1998.

Optimization of Model Structure

- Proposed by *Optimizing Parameters of Multi-Layer Convolutional Neural Network by Modeling and Optimization Method*.
- **Optimizing procedures**
  1. **Parameter Selection:** Main structure, the optimized hyperparameters, and levels selection.
  2. **Design experiments:** using uniform experimental design (UED).
  3. **Data Acquisition**: Experimental data acquiring.
  4. **Model Development**: between hyperparameters and performance (mean absolute percentage error, MAPE).
     $$\text{error} = f_{error}(\text{hyperparameters}) \quad (1)$$
  5. **Optimization:** by full-factorial searching algorithm. (Minimize the MAPE of models)
     $$\text{fitness} = \text{MAPE} = f_{MAPE}(\text{hyperparameters}) \quad (2)$$
  6. **Verification**
- **Particle swarm optimization (PSO)** is applied to compare with full-factorial searching algorithm in the thesis.

"Optimizing parameters of multi-layer convolutional neural network by modeling and optimization method," *IEEE Access*, vol. 7, pp. 68316-68330, 2019.

Particle swarm optimization for optimization

- Min MAPE

  s.t. hyperparameters

- Using surrogate model developed by neural network

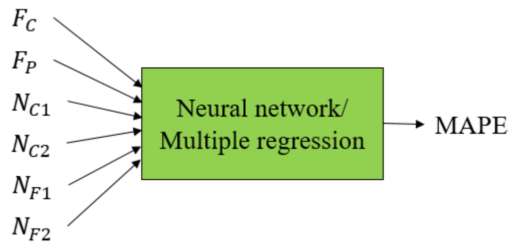

$$P_i(t+1) = P_i(t) + V_i(t+1)$$

$$V_i(t+1) = w \times V_i(t) + \text{random} \times c_1 \times \left(P_{pbest} - P_i(t)\right) + \text{random} \times c_2 \times \left(P_{gbest} - P_i(t)\right)$$

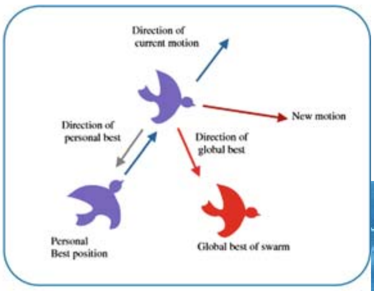

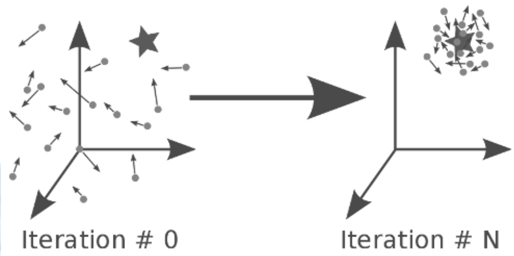

CNN for Prediction: Machining Quality Prediction (1/9)

- **Dataset** introduction
  - The dataset is proposed in [R1].
  - Tungsten carbide milling cutter are used to cut S45C steel.
  - The accelerometers are mounted on the spindle and vise to measure the vibrations in *X, Y,* and *Z* direction.
  - The sampling frequency is 10 kHz.
  - The surface roughness is measured by Mitutoyo SV-C3200S4.
  - There are total 153 data.

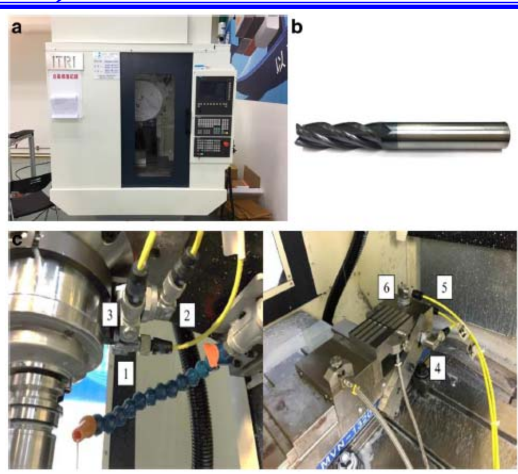

✓ (a) Milling machine of experiment. (b) Tungsten carbide milling cutter. (c) Setup of accelerometers on spindle and vise.

[R1] K. W. Lei and T. Y. Wu, "Prediction of surface roughness in milling process using vibration signal analysis and artificial neural network," *The International Journal of Advanced Manufacturing Technology* **volume 102**, pages305–314(2019) http://web.nchu.edu.tw/~tianyauwu/data/ra_s45c/ra_s45c.htm

CNN for Prediction: Machining Quality Prediction (2/9)

- **3 axial vibration signals of vise** are applied as inputs.
- A 1DCNN with parallel convolutional structure is applied to predict machining quality. The features of vibration signals in X, Y, Z axis are extracted separately.
- The optimization for CNN structure is applied in this application.

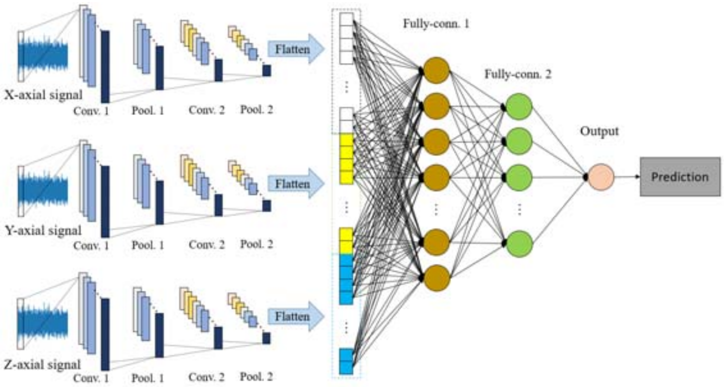

◆ The structure of CNN for predicting machining quality.

◆ Hyperparameters of 1DCNN for predicting machining quality.

Layers	Filter size	Stride	Number of Filters or nodes	Activation function
Conv. 1 (X, Y, Z)	F_C (16~25)	2	N_{C1} (11~20)	ReLU
Pool. 1 (X, Y, Z)	F_P (11~20)			
Conv. 2 (X, Y, Z)	F_C (16~25)	2	N_{C2} (11~20)	ReLU
Pool. 2 (X, Y, Z)	F_P (11~20)			
Flatten				
Fully-connected 1			N_{F1} (10~100)	ReLU
Fully-connected 2			N_{F2} (10~100)	ReLU
Output			1	None

CNN for Prediction: Machining Quality Prediction (3/9)

- There are six design factors. Four levels are selected for each factors. The uniform layout applied here is $U_{28}(4^6)$.
  - ➢ The selection of hyperparameters are based on [R2].
  - ➢ The structure is based on the performance of predicting model using single axial signals.
  - ➢ Selection of F_C, F_P, N_{C1}, N_{C2}: **The number of features after flatten layer is close to the number of nodes in the first fully-connected layer.**
- Every structure is tested for three times.

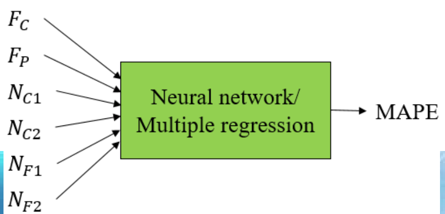

◆ MAPE of CNN with design factors predicting machining quality.

F_C	F_P	N_{C1}	N_{C2}	N_{F1}	N_{F2}	Avg. testing MAPE	Std.
16	17	14	17	100	70	14.35	0.539258751
25	20	17	14	100	40	13.57	3.270045871
19	17	17	17	70	40	16.00333333	3.239140833
16	14	11	20	100	40	18.42666667	4.279746877
19	14	17	11	40	70	18.3	3.296922808
16	20	11	11	10	70	23.83333333	1.909589834
22	11	17	20	40	10	25.16	6.573271636
22	17	17	11	10	100	23.11333333	1.005700419
16	14	17	14	10	10	24.25666667	2.892772603
22	20	14	14	40	70	19.11	4.725007937
25	14	20	14	70	70	15.17333333	1.84819732
19	11	11	17	10	70	25.44	5.371787412
25	**11**	**17**	**20**	**100**	**70**	**11.33666667**	**2.476051965**
19	20	20	11	100	10	18.82666667	4.710141541
16	11	20	17	40	40	18.46333333	1.602789235
22	11	11	14	10	40	21.03	2.205833176
22	14	11	11	70	100	18.4	5.753885644
25	17	20	11	40	40	16.59333333	3.317368435
16	17	20	20	70	100	13.68333333	2.2251367
25	20	11	17	70	100	18.50333333	4.724683411
25	14	14	17	40	100	18.52333333	2.156161713
25	17	14	20	10	10	19.17333333	4.337998771
22	14	20	17	100	10	16.02333333	1.626939868
19	17	11	14	40	10	19.54333333	5.028323113
19	11	14	14	100	100	15.81	0.610245852
16	11	14	11	70	10	28.36333333	7.945264837
22	20	14	20	70	40	15.21333333	2.673131746
19	20	20	20	10	100	18.87666667	2.240186004

[R2] "Optimizing parameters of multi-layer convolutional neural network by modeling and o... *IEEE Access*, vol. 7, pp. 68316-68330, 2019.

CNN for Prediction: Machining Quality Prediction (4/9)

- **Model Development**
- At first, **multiple regression (MR)** is applied for modeling the relation between hyperparameters and corresponding performance.
- The hyperparameters and MAPE are normalized.

- $$\text{MAPE} = 0.851765 - 0.327610F_C - 0.416407F_P + 0.014152N_{C1} + 0.237988N_{C2} + 0.124956N_{F1} - 0.279920N_{F2} + 0.059016F_C N_{F2} + 0.252224F_C N_{C2} - 0.222143F_P N_{C2} + 0.732162F_P N_{F2} - 0.335637N_{C1}N_{C2} - 0.045989N_{C1}N_{F2} - 0.476843N_{C2}N_{F1} - 0.309332N_{F1}N_{F2} \quad (3)$$

- *R*-squared: 0.9061

CNN for Prediction: Machining Quality Prediction (5/9)

- Full-factorial searching algorithm is applied for optimization.
- The optimized hyperparameters combination of **MR model**
  - F_C: 25
  - F_P: 20
  - N_{C1}: 20
  - N_{C2}: 20
  - N_{F1}: 100
  - N_{F2}: 10
  - Corresponding MAPE: 5.788%

◆ Testing MAPE of the optimized hyperparameters combination using MR model.

Test MAPE 1	Test MAPE 2	Test MAPE 3	Avg. MAPE	Standard deviation
15.74%	13.97%	13.19%	14.3%	1.090%

- The optimized hyperparameters combination is verified **three times**.
- The prediction has 147.06% of error.
- The hyperparameters combination does not perform better comparing to the UED experiments.

CNN for Prediction: Machining Quality Prediction (6/9)

- **Model Development**
- A **neural network (NN)** is applied for modeling the relation between hyperparameters and corresponding performance.
- The hyperparameters and MAPE are normalized.
- Initial learning rate: 0.005
- R-squared: 0.9999999996

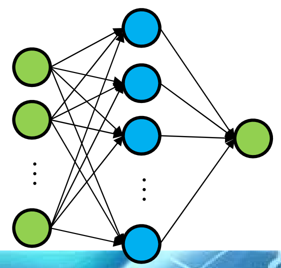

◆ Structure of NN for modeling the relation between factors and testing MAPE.

Layer	Nodes	Activation function	Bias
Input	6	None	None
Hidden 1	12	Sigmoid	None
Output	1	None	Yes
Total parameters	85		

CNN for Prediction: Machining Quality Prediction (7/9)

- **Optimization: *Full-factorial searching algorithm***
- The optimized hyperparameters combination of **NN model**
  - ➢ F_C: 25
  - ➢ F_P: 11
  - ➢ N_{C1}: 18
  - ➢ N_{C2}: 12
  - ➢ N_{F1}: 100
  - ➢ N_{F2}: 50
  - ➢ Corresponding MAPE: 10.849%

◆ Testing MAPE of the optimized hyperparameters combination using NN model.

Test MAPE 1	Test MAPE 2	Test MAPE 3	Avg. MAPE	Standard deviation
11.04%	10.68%	8.44%	10.053%	1.150%

- The optimized hyperparameters combination is verified **three times**.
- The prediction has 7.337% of error.
- **The optimized structure improves the performance by 11.3%.**

CNN for Prediction: Machining Quality Prediction (8/9)

- **Optimization:** PSO
  - Iterations: 3000 (Early stop criteria: P_{gbest} stops revolving for 500 iteration.)
  - Particles: 250
- The optimized result of NN model
  - F_C: 25
  - F_P: 11
  - N_{C1}: 18
  - N_{C2}: 12
  - N_{F1}: 100
  - N_{F2}: 50

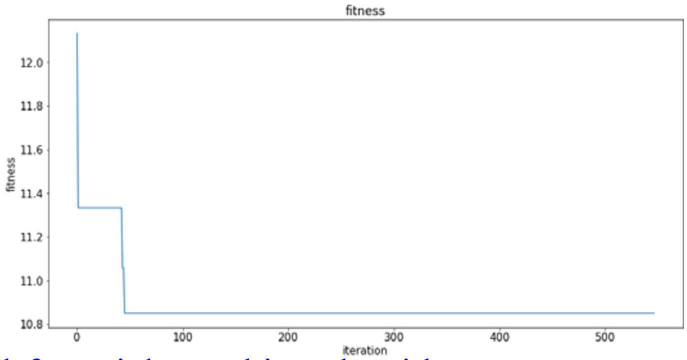

- The optimized result is the same as full-factorial searching algorithm.
- **PSO takes 43.435 seconds to complete the process while 146.87 seconds for full-factorial searching algorithm.**

CNN for Prediction: Machining Quality Prediction (9/9)

- The results show that neural network can be applied for modeling. The **structure, learning rate**, and **normalization or not** affect the performance of neural network and the final optimized result a lot.
  - A **simple NN with smaller learning rate** is recommended.
  - **Normalization** is necessary.
- When the structure of optimized **CNN is more complex**, **PSO and other optimization methods are necessary** to reduce the needed time.
- MAPE of machining quality prediction using CNN is **10.053%** while the MAPE of neural network using characteristics of vibration signals in [R1] is **18%**.

CNN for Classification: Bearing Faults Classification (1/3)

- Dataset: Case Western Reserve University (CWRU) bearing data https://csegroups.case.edu/bearingdatacenter/pages/apparatus-procedures
- Signals are collected using accelerometers mounted at the drive end of the motor with 12 kHz of sampling frequency.
- Faults are man-made using electrical-discharge machine.
- 64 data in the dataset.
  - Use sliding window to increase the number of dataset.
    - 1657 for training, 711 for testing

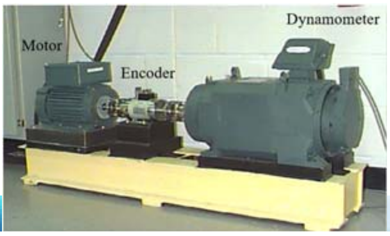

✓ Test stand of CWRU bearing data.

Inner ring fault

Outer ring fault

Ball fault

◆ Characteristic frequencies under different rotating speed.

Rotating speed (rpm)	Freqs. (Hz)	F_{BPO}	F_{BPI}	$2F_{BS}$	F_C
1797		107.364	162.186	141.168	11.929
1772		105.870	159.930	139.204	11.763
1750		104.556	157.944	137.468	11.617
1730		103.361	156.139	135.904	11.485

CNN for Classification: Bearing Faults Classification (2/3)

- Use **vibration signals** as inputs of **1DCNN**.
- Both training and testing accuracy are **100%**.

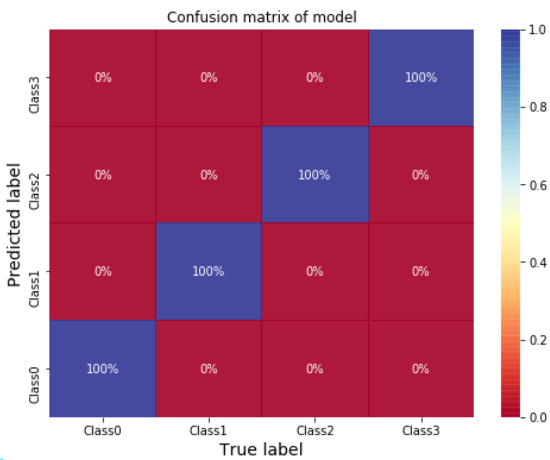

✓ Confusion matrix of 1DCNN model for classifying CWRU bearing data.

◆ Structure of 1DCNN for bearing faults classification using vibration signals.

Layer	Filter size	Stride	Number of filters of nodes	Activation func.
Conv. 1	30	1	8	ReLU
Pool. 1	4			
Conv. 2	30	1	16	ReLU
Pool. 2	4			
Conv. 3	30	1	32	ReLU
Pool. 3	4			
Conv. 4	30	1	64	ReLU
Pool. 4	4			
Flatten				
Fully-Conn. 1			128	ReLU
Fully-Conn. 2			32	ReLU
Output			4	Softmax
Total parameters	388488			

CNN for Classification: Bearing Faults Classification (3/3)

- Use **short-time Fourier transform (STFT) time-frequency spectra** as inputs of **2DCNN**.
- The axes of images are removed when input into the model.
- Both training and testing accuracy are **100%**.

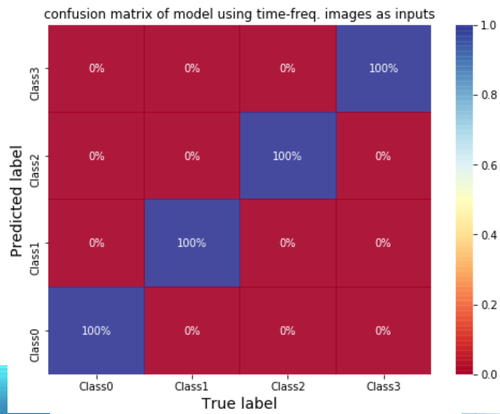

✓ Confusion matrix of 2DCNN model for classifying CWRU bearing data.

◆ Structure of 2DCNN for bearing faults classification using time-frequency spectra.

Layer	Filter size	Stride	Number of filters of nodes	Activation func.
Conv. 1	9 × 9	2 × 2	4	ReLU
Conv. 2	9 × 9	2 × 2	8	ReLU
Pool. 1	4 × 4			
Conv. 3	4 × 4	2 × 2	16	ReLU
Conv. 4	4 × 4	2 × 2	32	ReLU
Pool. 4	2 × 2			
Flatten				
Fully-Conn. 1			64	ReLU
Fully-Conn. 2			32	ReLU
Output			4	Softmax
Total parameters	63622			

CNN for Classification: Tool Wear Classification (1/2)

- **Dataset** introduction
  - Milling machine: CHMER HM4030L
  - Tungsten carbide milling cutters with 6 mm of diameter are used to mill S45C steel.
  - A tri-axial accelerometer (CTC AC230) is mounted on the spindle.
  - The sampling rate is 100 kHz.
  - The tool wear is measured by Camera (Deryuan RS-500), ImageJ, and PhotoImpact.

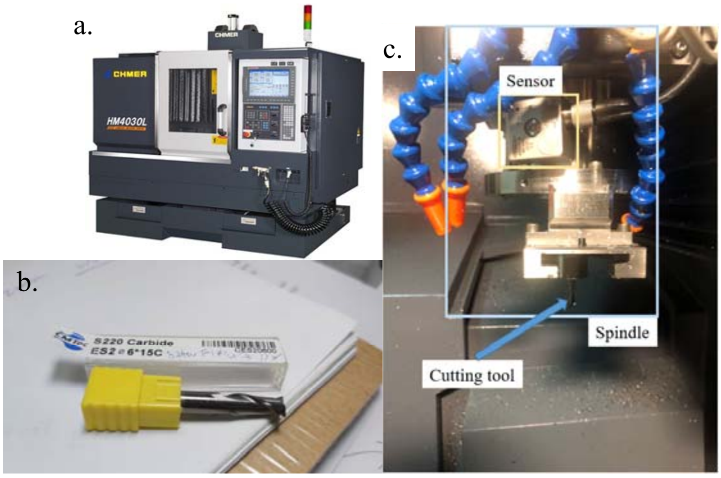

✓ (a) Milling machine of experiment.
(b) Tungsten carbide milling cutter (2 blades).
(c) Setup of accelerometers on spindle.

CNN for Classification: Tool Wear Classification (2/2)

- Use **STFT time-frequency spectra of Y-axial signals** as inputs of **2DCNN**.
  - There are total 742 data (unworn: 504, worn: 238), 371 for training and 371 for testing.
- The axes of images are removed when input into the model.
- Both training and testing accuracy are 100%.

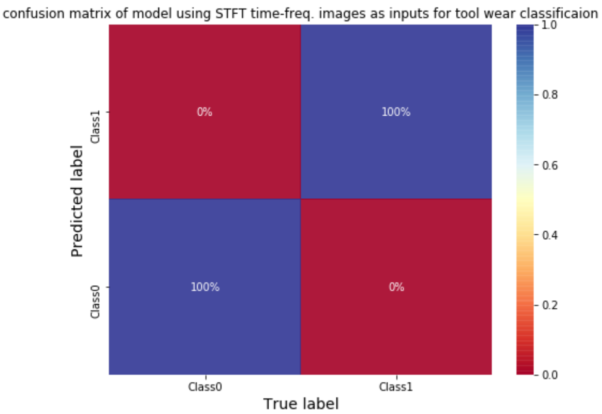

✓ Confusion matrix of 2DCNN model for classifying tool wear.

◆ Structure of 2DCNN for tool wear classification using time-frequency spectra.

Layer	Filter size	Stride	Number of filters of nodes	Activation func.
Conv. 1	9 × 9	2 × 2	4	ReLU
Conv. 2	9 × 9	2 × 2	8	ReLU
Pool. 1	4 × 4			
Conv. 3	4 × 4	2 × 2	16	ReLU
Conv. 4	4 × 4	2 × 2	32	ReLU
Pool. 4	2 × 2			
Flatten				
Fully-Conn. 1			64	ReLU
Fully-Conn. 2			32	ReLU
Output			2	Softmax
Total parameters	28360			

Summary of Applications of CNN for Vibration Signal Analysis

- The **vibration signals** can be applied for classification and prediction **directly** or combined with **signal processing techniques**.
- CNN can **extract features** in vibration signals and time-frequency spectra **automatically**.
- By **optimizing structure** of CNN, a better performance of model can be achieved. The optimized results are highly relative to modeling.

Outlines

- Introduction
- Literatures review
- Applications of CNN for vibration signals
- **Explainable Artificial Intelligence (XAI) for Vibration Signals Analysis: Bearing Faults Classification Using CNNs**
  - Gradient Class Activation Mapping (Grad-CAM)
  - Explanation Using STFT Time-Frequency Spectra of CWRU Bearing Data
  - Observation of Attention Maps
  - Verification of Explanations
  - Verification of Methodology Using Tool Wear Classification
- Conclusions
- Future Researches

Attention-based method- Grad-CAM

- 顱內出血診斷

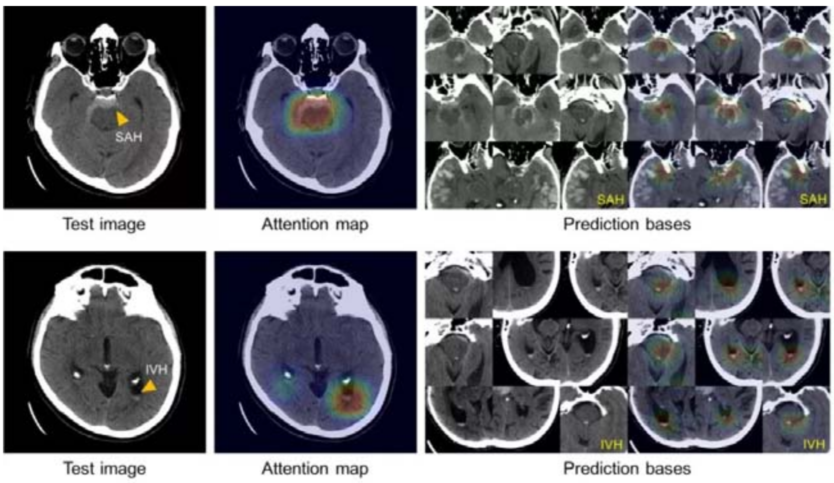

https://www.jiqizhixin.com/articles/2018-12-26

- 即時螺紋檢測

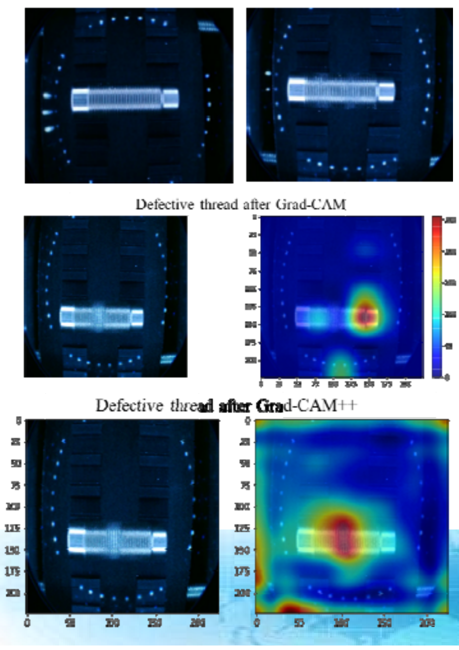

Gradient class activation mapping (Grad-CAM)

- Function: computing the attention of model.
- The oth feature map

$$F^o = \frac{1}{Z}\sum_m \sum_n A^o_{m,n}$$

  - Z: the number of pixels in the feature map
  - m, n: the index of row and column of the feature map
  - $A^o_{m,n}$: the value of pixel in the mth row and nth column.
- The attention map $Y^C = \sum_o \alpha^C_o F^o$
  - α^C_o: the weight of the oth feature map

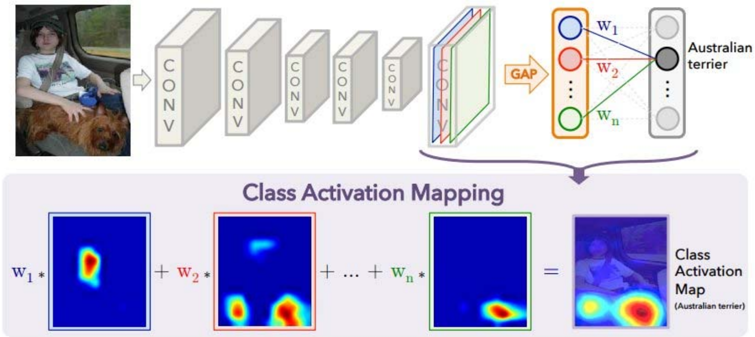

Gradient class activation mapping (Grad-CAM)

- By partial differentiation and simplification, α^C_o can be computed by

$$\alpha^C_o = \sum_m \sum_n \frac{\partial Y^C}{\partial A^o_{m,n}}$$

- The attention map without normalization can be represented as

$$Y^C = \sum_m \sum_n \sum_o \alpha^C_o A^o_{m,n}$$

- The normalized attention map computed using Grad-CAM can be represented as

$$S = \frac{1}{Z}\sum_m \sum_n \sum_o \alpha^C_o A^o_{m,n}$$

XAI- Attention Map

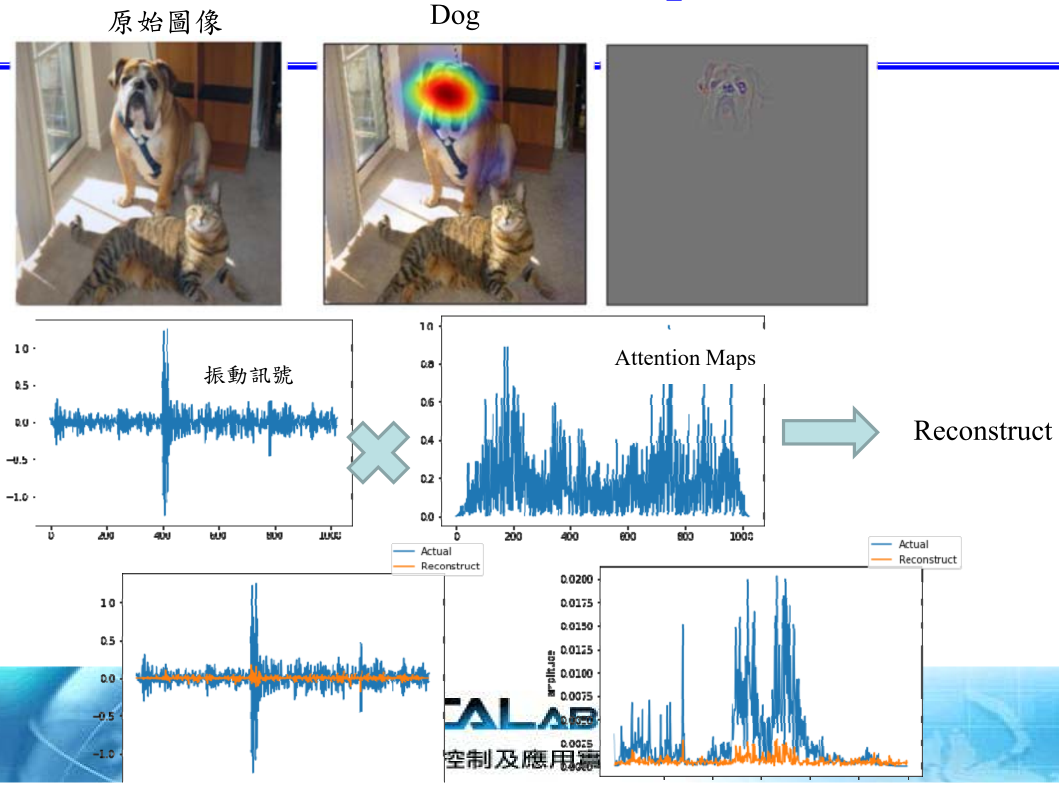

Explainable AI for Raw Data (vibration Signals) using 1DCNN

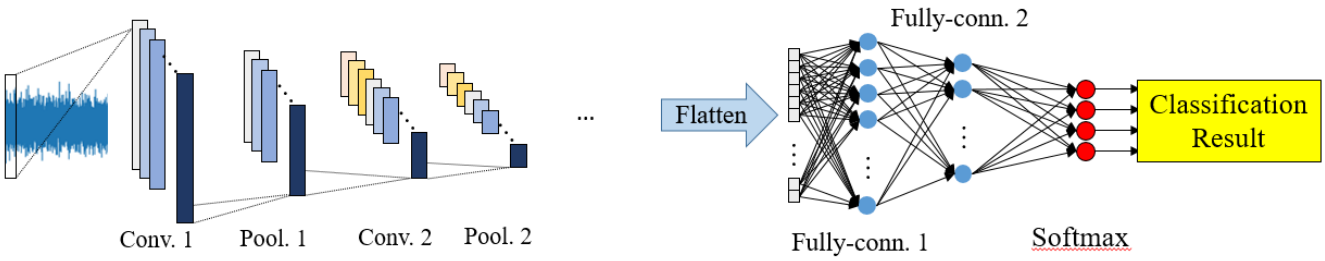

Explainable AI for Raw Data Analysis

- Testing accuracy of model: 100%
- attention signal = attention × original signal
- Analyzing attention of model using a normal bearing.

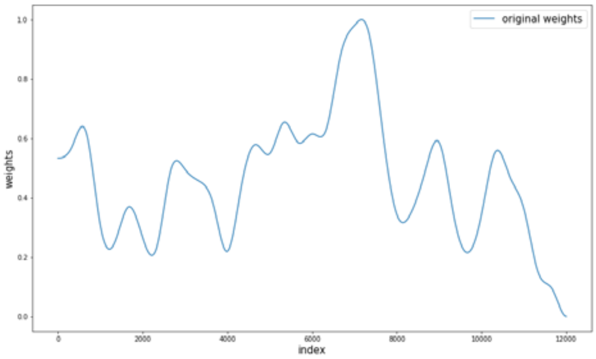

◆ Attention of model using vibration signal of a normal bearing under 1797 rpm.

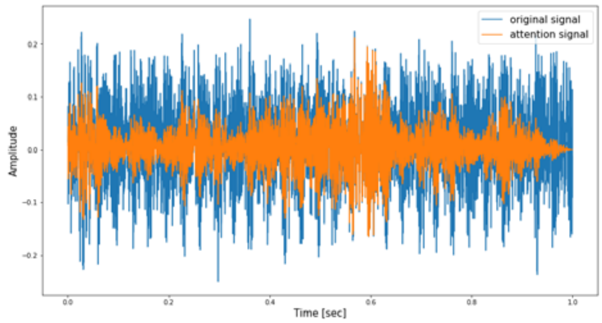

◆ Comparison between attention signal and original signal of a normal bearing under 1797 rpm.

Explanation of model using raw signals

- Analyzing attention of model using a normal bearing.

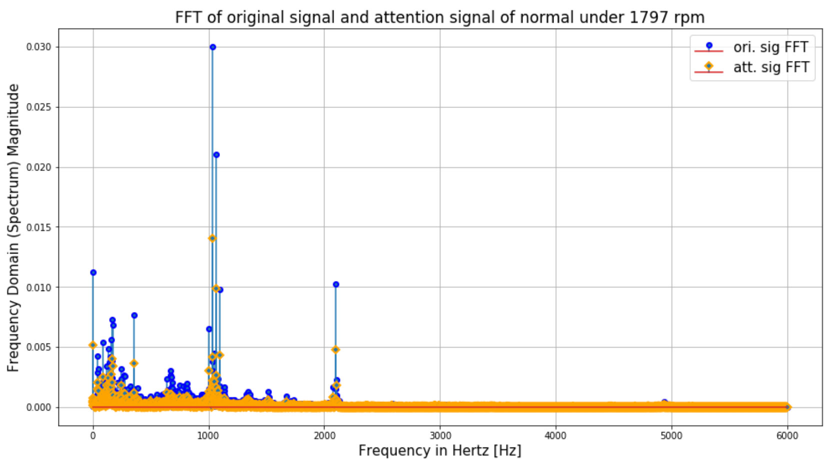

Explanation of model using raw signals

- Analyzing attention of model using a bearing with inner ring fault.

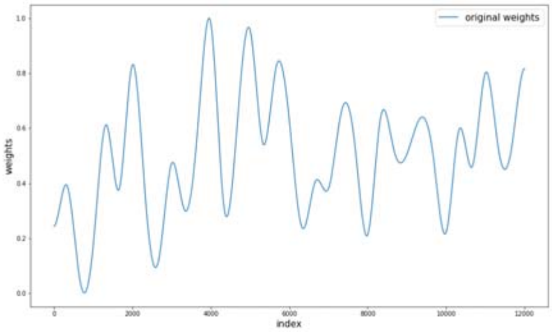

◆ Attention of model using vibration signal of a bearing with inner ring fault under 1797 rpm.

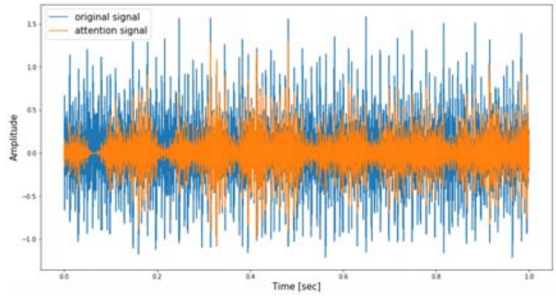

◆ Comparison between attention signal and original signal of a bearing with inner ring fault under 1797 rpm.

Explanation of model using raw signals

- Analyzing attention of model using a bearing with inner ring fault.

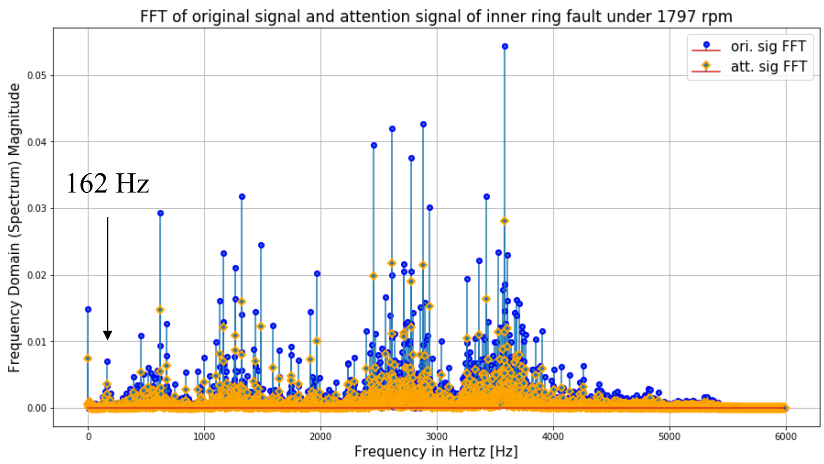

Explanation of model using raw signals

- Analyzing attention of model using a bearing with outer ring fault.

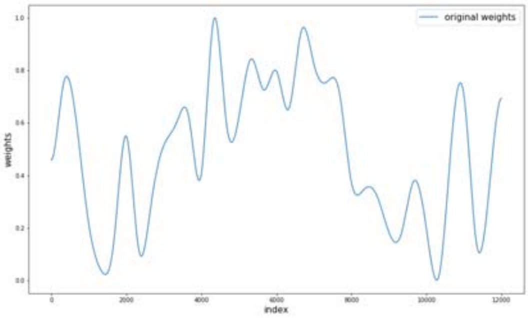

◆ Attention of model using vibration signal of a bearing with outer ring fault under 1797 rpm.

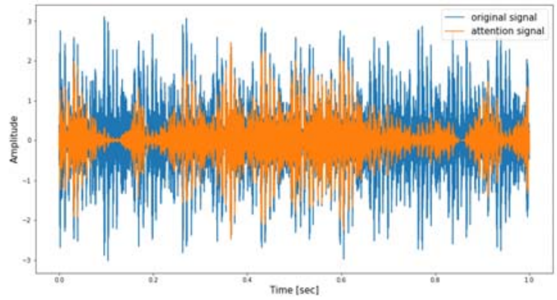

◆ Comparison between attention signal and original signal of a bearing with outer ring fault under 1797 rpm.

Explanation of model using raw signals

- Analyzing attention of model using a bearing with outer ring fault.

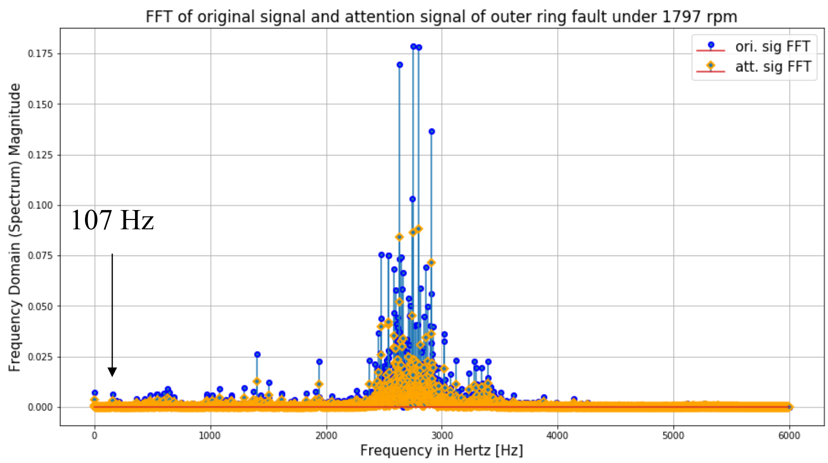

Explanation of model using raw signals

- Analyzing attention of model using a bearing with ball fault.

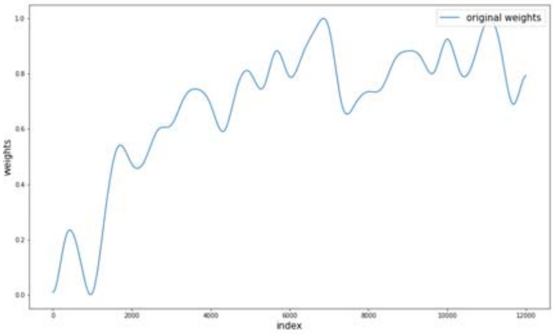

◆ Attention of model using vibration signal of a bearing with ball fault under 1797 rpm.

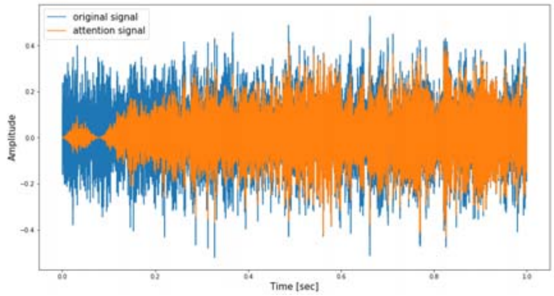

◆ Comparison between attention signal and original signal of a bearing with ball fault under 1797 rpm.

Explanation of model using raw signals

- Analyzing attention of model using a bearing with ball fault.

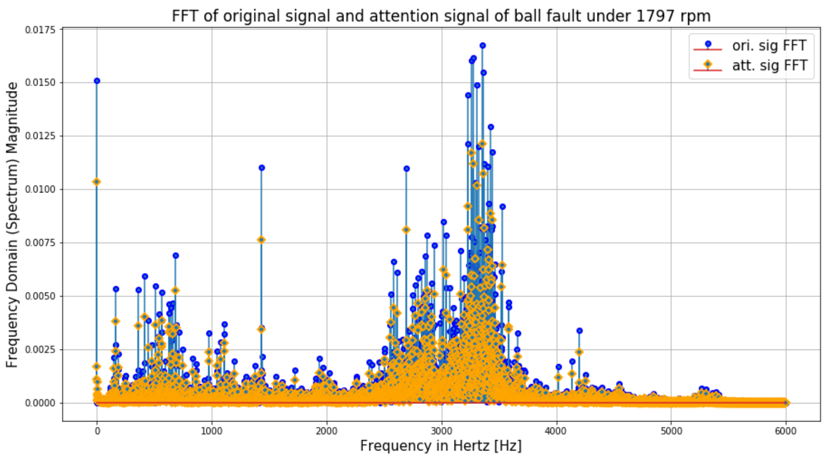

Explanation of model using raw signals

- The attention of 1DCNN cannot be observed directly.
  - Applying frequency spectra to analyze the frequency distribution of attention.
  - The expl

Process of Grad-CAM

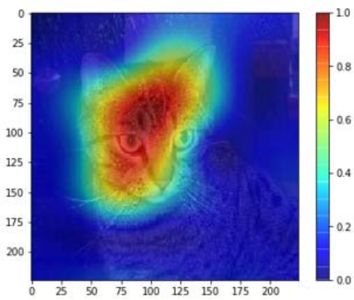

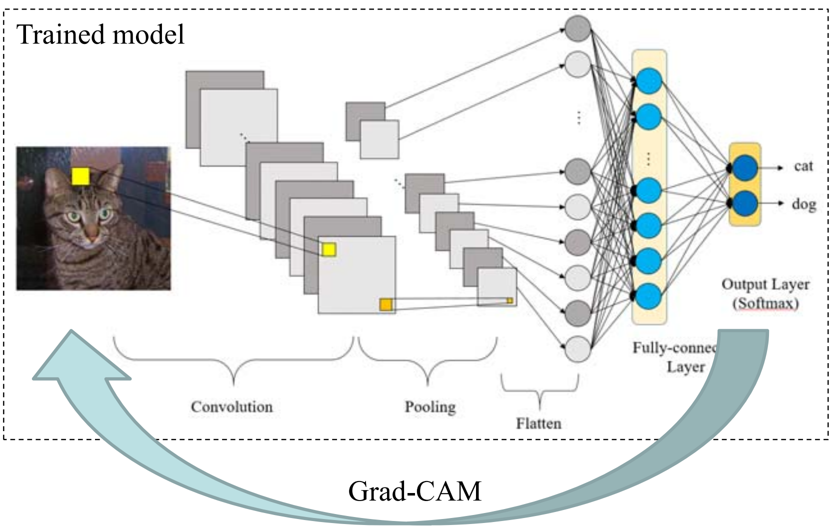

Some examples of using Grad-CAM

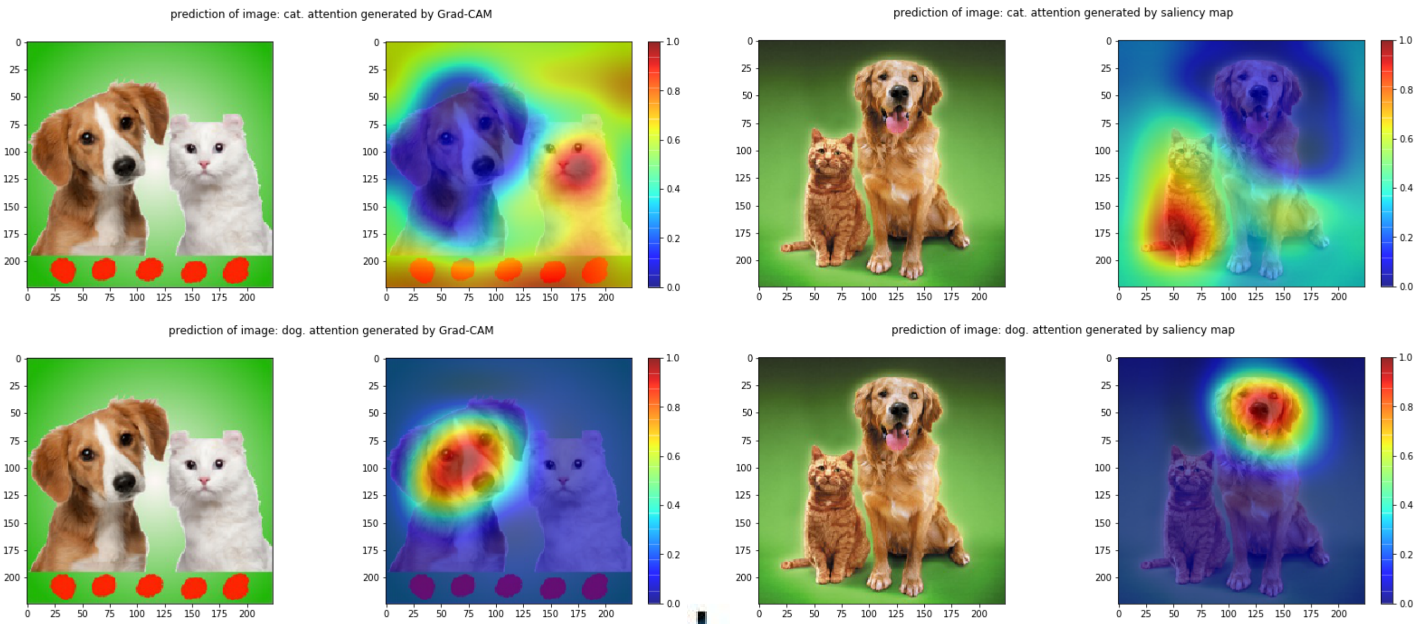

Some examples of using Grad-CAM

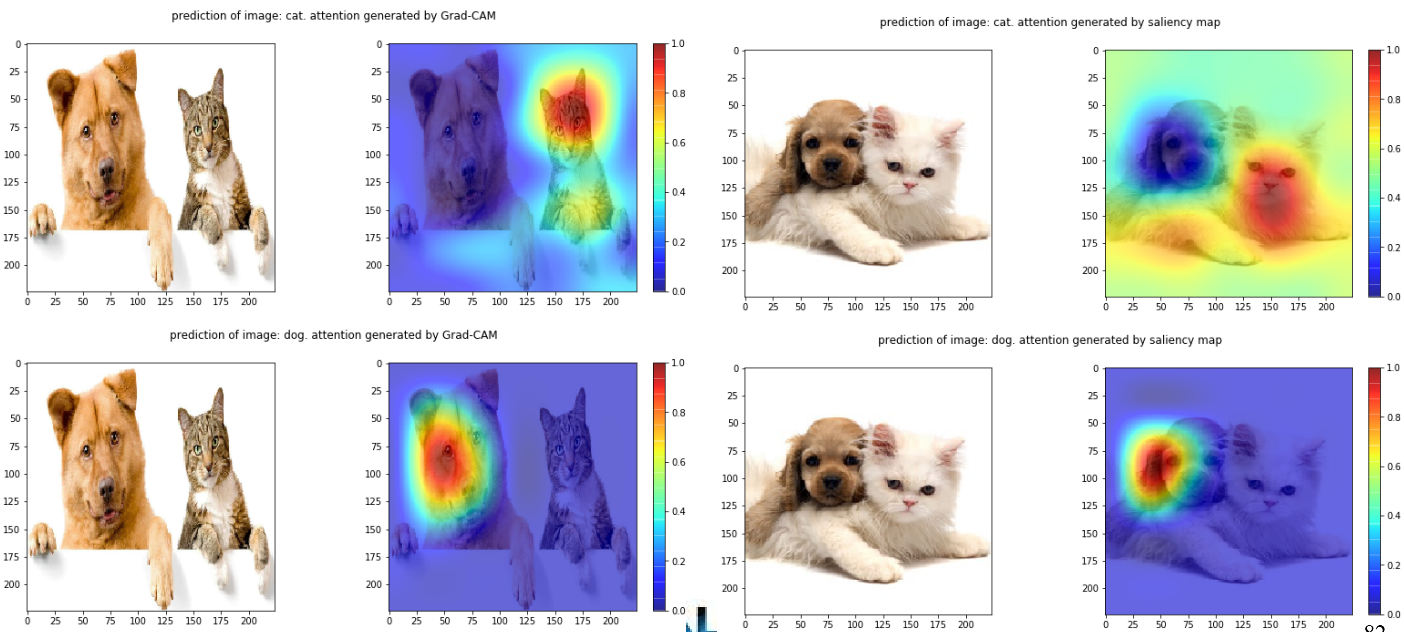

Explanation of model using time-frequency spectra (2DCNN)

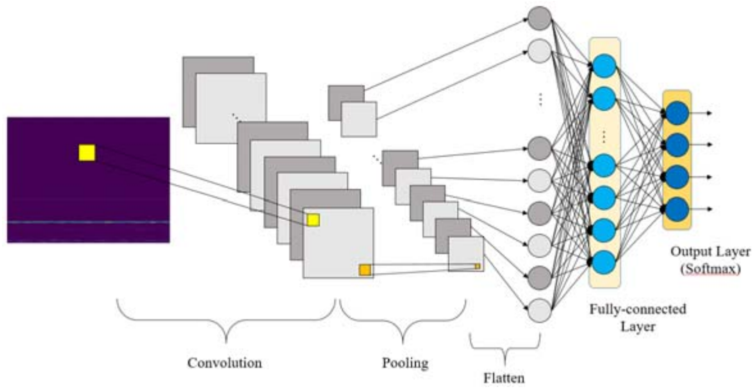

Explanation Using STFT Time-Frequency Spectra of CWRU Bearing Data (1/4)

- The model is mentioned in applications of 2DCNN with 100% of testing accuracy.
- The comparison between using vibration signals, STFT time-frequency spectra, and wavelet transform (WT) time-frequency spectra is also carried out.

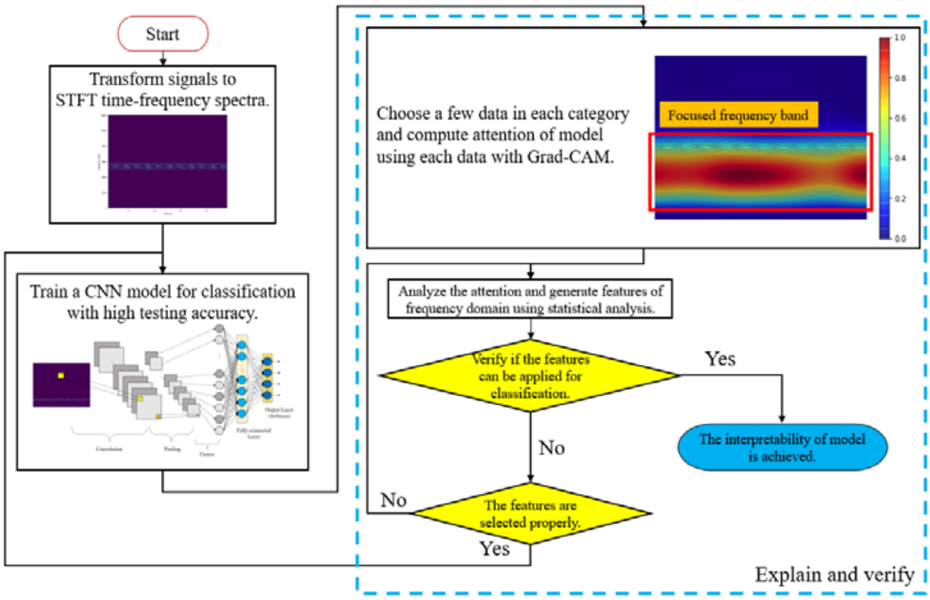

Explanation Using STFT Time-Frequency Spectra of CWRU Bearing Data (2/4)

- The attention maps of model are overlapped with input images.

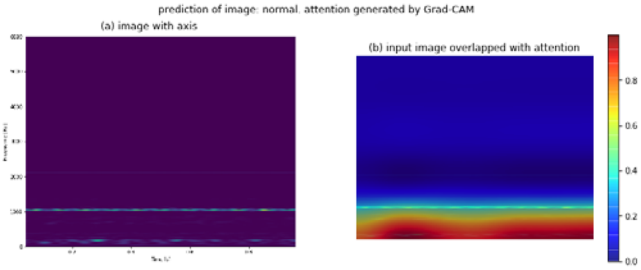

✓ The attention map of model using a normal bearing.

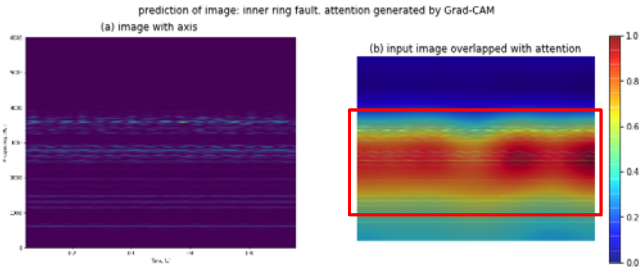

✓ The attention map of model using a bearing with inner ring fault.

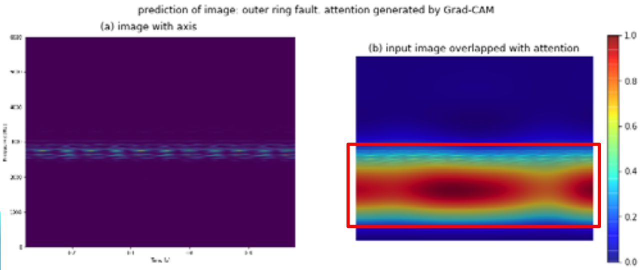

✓ The attention map of model using a bearing with outer ring fault.

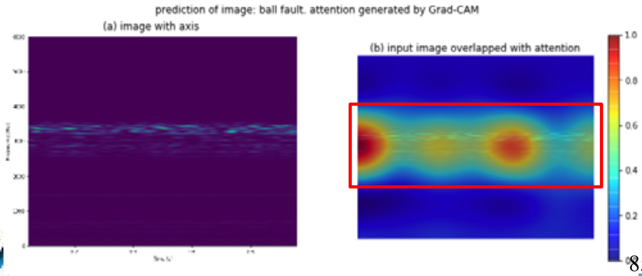

✓ The attention map of model using a bearing with ball fault.

Spectrum Union and Observation

Explanation Using STFT Time-Frequency Spectra of CWRU Bearing Data (3/4)

- The attention of model using a normal bearing shows that the model focuses at low-frequency band since there is no obvious structure resonance for a normal bearing.

- The attentions of model with damaged bearings show that **the model focuses at high-frequency bands from about 1000 to 4000 Hz which are cause by structure resonance** but **not the characteristic frequencies** [R3, R4].

[R3] G. Zhang, Y. Zhang, T. Zhang, and R. Mdsohel, "Stochastic resonance in an asymmetric bistable system driven by multiplicative and additive Gaussian noise and its application in bearing fault detection," *Chinese Journal of Physics*, vol. 56, no. 3, pp. 1173-1186, 2018.

[R4] Q. He, J. Wang, Y. Liu, D. Dai, and F. Kong, "Multiscale noise tuning of stochastic resonance for enhanced fault diagnosis in rotating machines," *Mechanical Systems and Signal Processing*, vol. 28, pp. 443-457, 2012.

Explanation Using STFT Time-Frequency Spectra of CWRU Bearing Data (4/4)

- The comparison between classifying using different inputs is sorted out.
- Hardware: NVIDIA Tesla V100 32GB GPU
- Environment: Python 3.6, Keras 2.2.4

Inputs	Computing time (average value using 5 times of experiment) Transforming time (sec/1 data)	Classifying time (sec/1 data)	Total computing time (sec/1 data)	Testing Accuracy	Input size	Explainable
Use raw vibration signals as inputs and explained using Grad-CAM	0	0.00133	0.00133	100%	12000*1	△
Use STFT spectra as inputs and explained using Grad-CAM	0.75258	0.00419	0.75677	100%	434*558*3	○
Using WT spectra as inputs and explained using Grad-CAM	**20.14071**	0.00394	20.14465	100%	278*558*3	×

Observation of Attention Maps (1/4)

- In order to compare the attentions of 1DCNN and 2DCNN, time-frequency spectra are spin 90° clockwise to match the X axis in frequency spectra of attention signals.

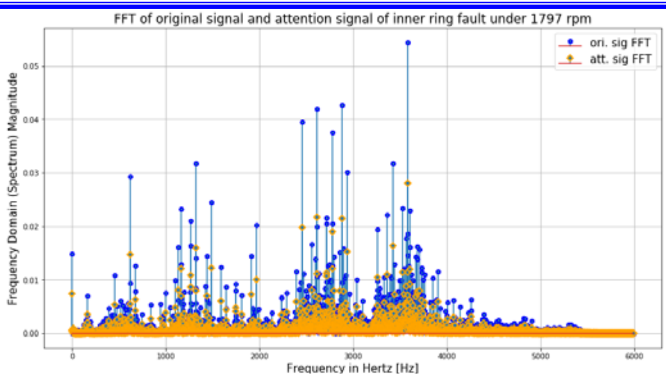

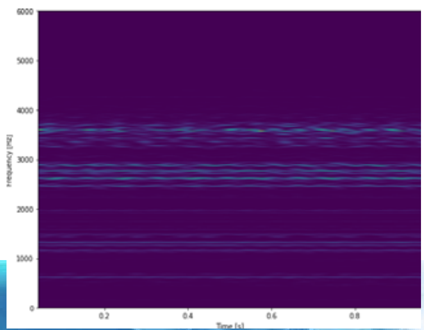

Spin 90° to match the frequency axis.

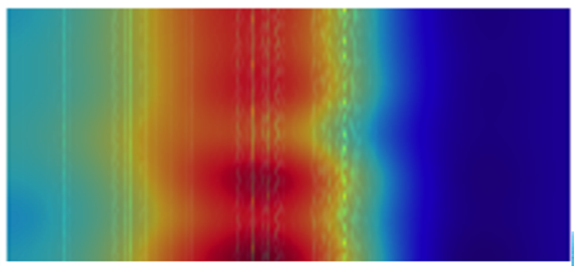

Observation of Attention Maps (2/4)

- Since there are no obvious structure resonance for normal bearings, both models focus at low-frequency bands.
- The attentions of a bearing with inner ring fault are focusing at 1000~4000 Hz.

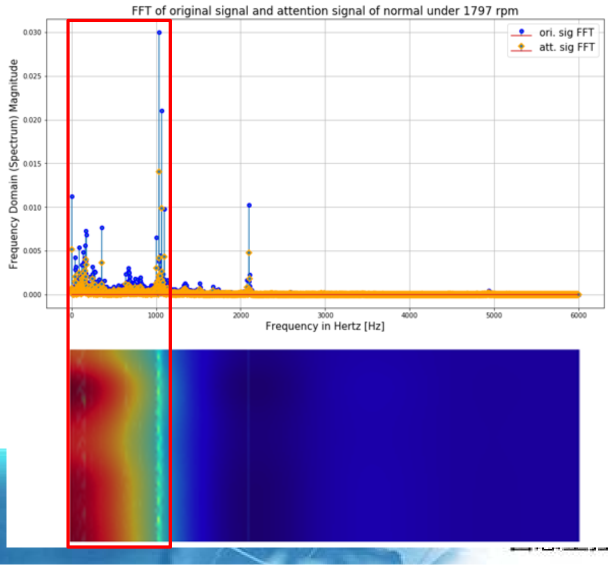

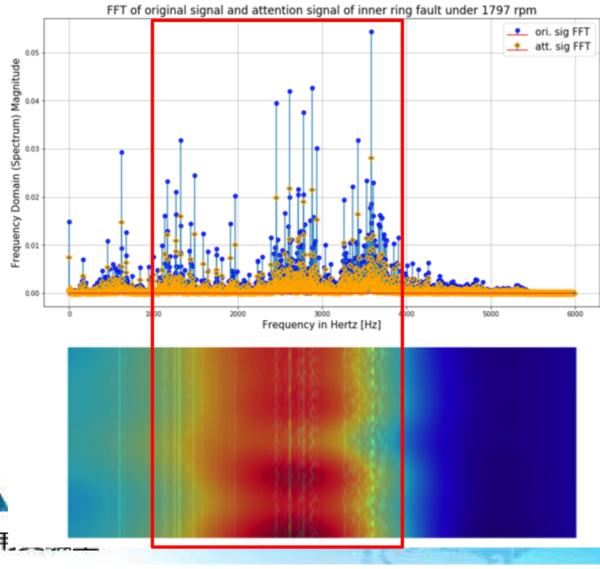

Observation of Attention Maps (3/4)

- The attentions of a bearing with outer ring fault are focusing at 800~3000 Hz.
- The attentions of a bearing with ball fault are focusing at 2000~4000 Hz.

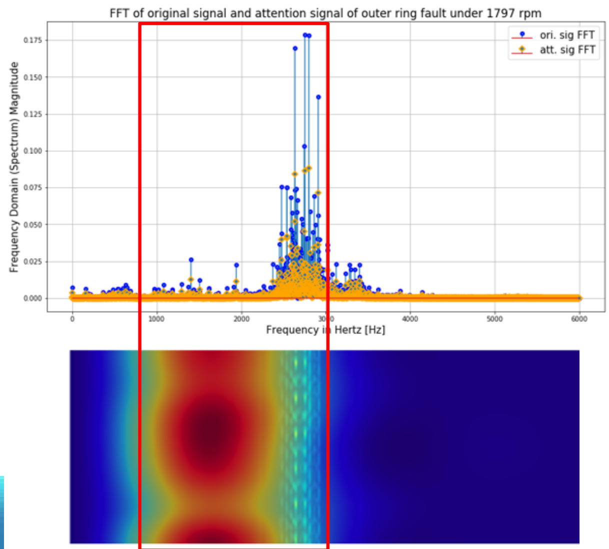

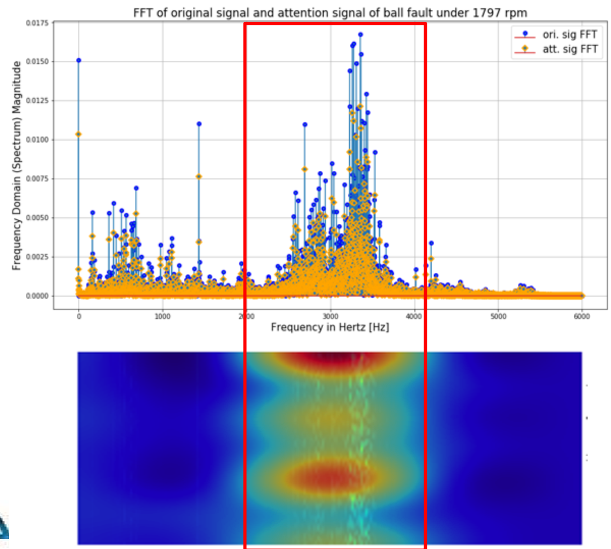

Observation of Attention Maps (4/4)

- The observation shows model focusing at high-frequency bands (1000~4000 Hz).
- By the observation, an assumption for explanation can be proposed: **The features in high-frequency band can be applied for classification more easily for the model instead of focusing at characteristic frequencies in diagnosis using signal processing methods**.
- The assumption is verified in next section.

Outlines

Features of High-Frequency Bands

- The observation of frequency distribution of bearings with different conditions in CWRU dataset is carried out.

✓ Average frequency spectrum of normal bearings.

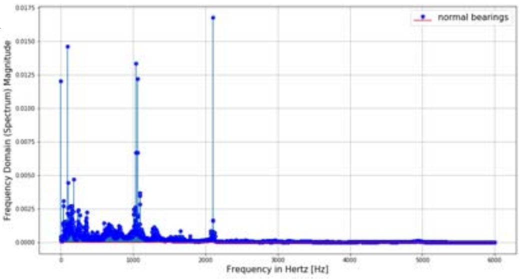

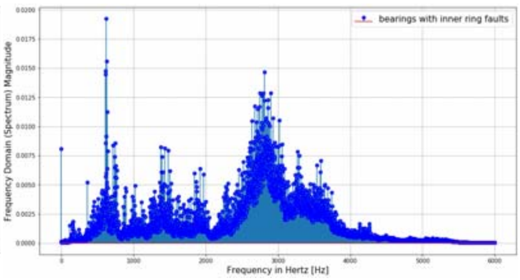

✓ Average frequency spectrum of bearings with inner ring faults.

✓ Average frequency spectrum of bearings with outer ring faults.

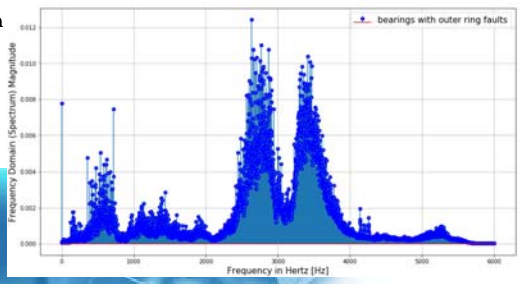

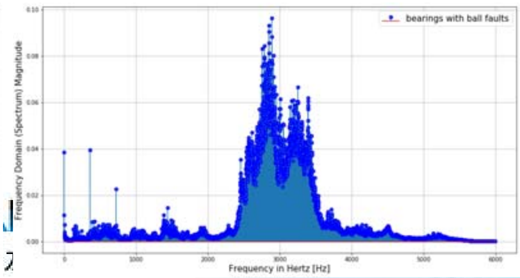

✓ Average frequency spectrum of bearings with ball faults.

Features of High-Frequency Bands

- The features in high-frequency bands are sorted out.
  - ➢ The average magnitude of 1001~2000 Hz
  - ➢ The average magnitude of 2001~3000 Hz
  - ➢ The average magnitude of 3001~4000 Hz
  - ➢ The kurtosis in 1001~2000 Hz
  - ➢ The kurtosis in 2001~3000 Hz
  - ➢ The kurtosis in 3001~4000 Hz
  - ➢ The skewness in 2001~3000 Hz
  - ➢ The skewness in 3001~4000 Hz
- The features are applied in verification of NN, ANFIS, and decision trees.

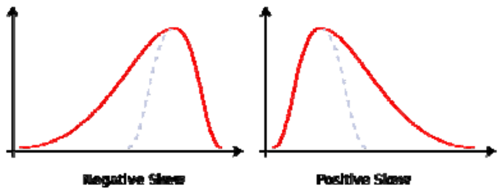

$$\text{skewness} = \frac{1}{N}\sum_{i=1}^{N}\frac{(x_i - \bar{x})^3}{\sigma^3}$$

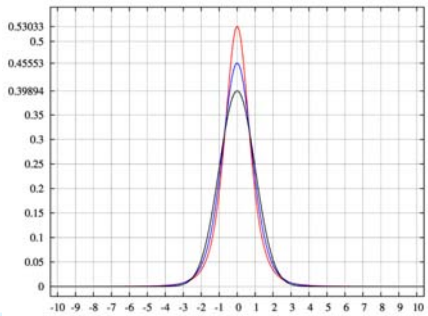

$$\text{kurtosis} = \frac{1}{N}\sum_{i=1}^{N}\frac{(x_i - \bar{x})^4}{\sigma^4}$$

Verification Using Neural Networks

- A simple NN is applied for verification.
  - Use the features in high-frequency bands as inputs of NN.
  - Both training and testing accuracy of model are 100%.

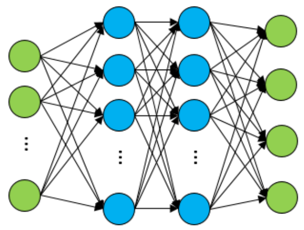

◆ Structure of NN for classifying bearing faults using features in high-frequency bands.

Layer	nodes	Activation function
Input layer	8	None
Hidden layer 1	10	Sigmoid
Hidden layer 2	10	Sigmoid
Output layer	4	Softmax

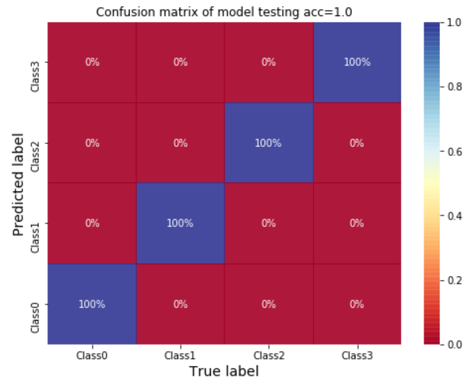

✓ Confusion matrix of NN for classifying bearing faults using features of high-frequency bands.

Verification Using ANFIS

- A first-order Sugeno-type ANFIS is applied in the thesis.
- 8 features in high-frequency bands are the inputs of ANFIS. 2 triangular membership function are applied for each input. → 256 rules
- Since ANFIS are mostly applied for prediction, the output of ANFIS is defined as class criteria.
  - The output values are rounded to match integer labels.
- The testing accuracy of ANFIS is 96.9%.

◆ Confusion matrix of ANFIS using testing data.

		Actual class			
		Normal	Inner ring	Outer ring	Ball
Predicted class	Ball	0	0	2	174
	Outer ring	0	5	322	15
	Inner ring	0	157	0	0
	Normal	35	0	0	0

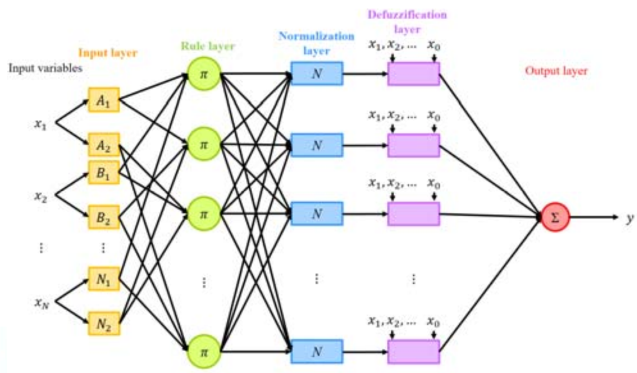

✓ Structure of ANFIS.

Decision Tree

- Decision tree is a simple algorithm mostly applied for classification.
- Structure of trees
  - Nodes
    - Root node: The start of the tree which contains entire dataset.
    - Internal nodes (decision nodes): The condition that can separate the dataset or subset into two subsets.
    - Leaf nodes: The final nodes of the tree.
  - Branches
- Information gain: The criteria for assessing and choosing the best decision.
  - Maximize the separated information. → Minimize the information gain of decisions.
  - Entropy

    $$\text{entropy} = \sum_c p_c \log_2 p_c \qquad (6)$$
  - Gini impurity

    $$\text{Gini Impurity} = \sum_c p_c(1 - p_c) = \sum(p_c - {p_c}^2) = 1 - \sum {p_c}^2 \qquad (7)$$

Verification Using Decision Tree

- Entropy is adopted as information gain.
- Skewness of 3001~4000 Hz is not applied in the tree.

✓ Decision tree for classification using features in high-frequency band. (Information gain: entropy)

Verification Using Decision Tree

- A NN is utilized to check if the feature is not necessary for classification.
- The training and testing accuracy are 100%.
- The result shows that the skewness of 3001~4000 Hz is not essential for classification using CWRU bearing dataset.

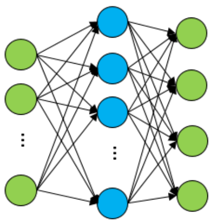

◆ Structure of NN for classifying bearing faults using features of high-frequency bands (without skewness of 3000~4000 Hz).

Layer	nodes	Activation function
Input layer	7	None
Hidden layer 1	10	Sigmoid
Output layer	4	Softmax

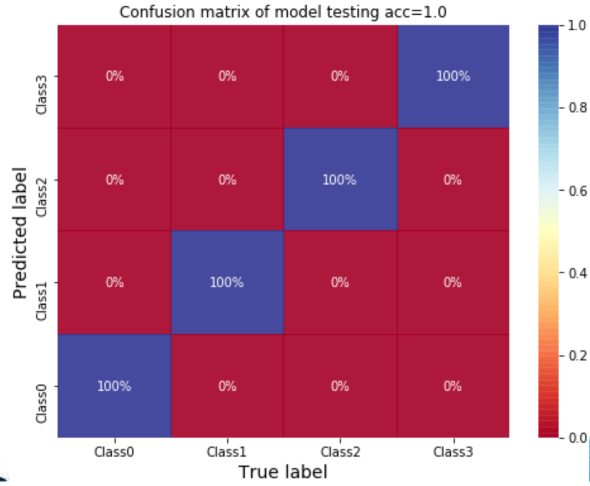

✓ Confusion matrix of NN for classifying bearing faults using features of high-frequency bands (without skewness of 3000~4000 Hz).

Comparison of Decision Tree and ANFIS Rules (1/2)

- Since all of the features need to be considered in ANFIS rules, a decision with more complete features is chosen.
- Prediction of ANFIS using a data which matches the decisions is 3.08 which belongs to outer ring fault.

	Normalize	
➢ Average 1k~2k Hz: 0.001050888		Average 1k~2k Hz: 0.1958
➢ Kurtosis 1k~2k Hz: 21.97054394		Kurtosis 1k~2k Hz: 0.01624
➢ Average 2k~2k Hz: 0.002055893		Average 2k~2k Hz: 0.07715
➢ Kurtosis 2k~2k Hz: 0.00205352		Kurtosis 2k~2k Hz: 0.09605
➢ Skewness 2k~3k Hz: 15.11562703		Skewness 2k~3k Hz: 0.01486
➢ Average 3k~4k Hz: 7.32406153		Average 3k~4k Hz: 0.0172
➢ Kurtosis 3k~4k Hz: 3.364888697		Kurtosis 3k~4k Hz: 0.07626
➢ Skewness 3k~4k Hz: 2.308279182		Skewness 3k~4k Hz: 0.06683

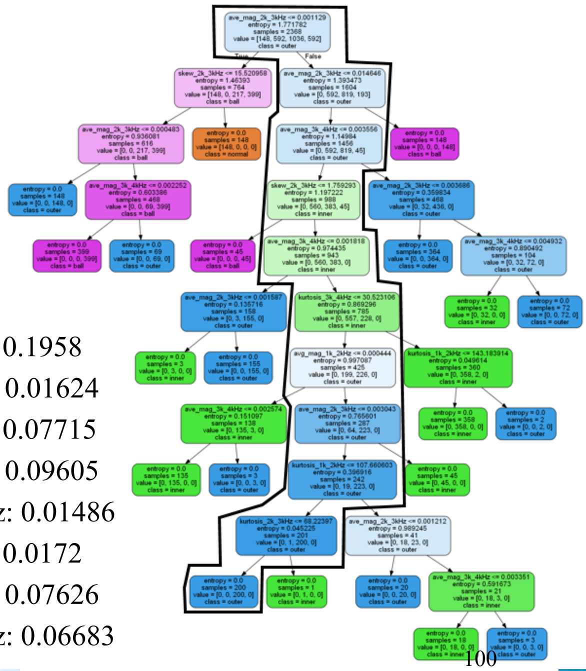

✓ The chosen decision of the decision tree.

Comparison of Decision Tree and ANFIS Rules (2/2)

- By observing the firing strength of ANFIS rules, the first rule has the largest firing strength.
- Rule 1: If (avg_1k is **low**) and (kur_1k is **low**) and (avg_2k is **low**) and (avg_3k is **low**) and (kur_2k is **low**) and (kur_3k is **low**) and (skew_2k is **low**) and (skew_3k is **low**) then (classes is [122.8173 6.2942 -92.7101 3.7964 272.4220 55.0627 -157.9949 -1.7471]×**X** +4.0015)

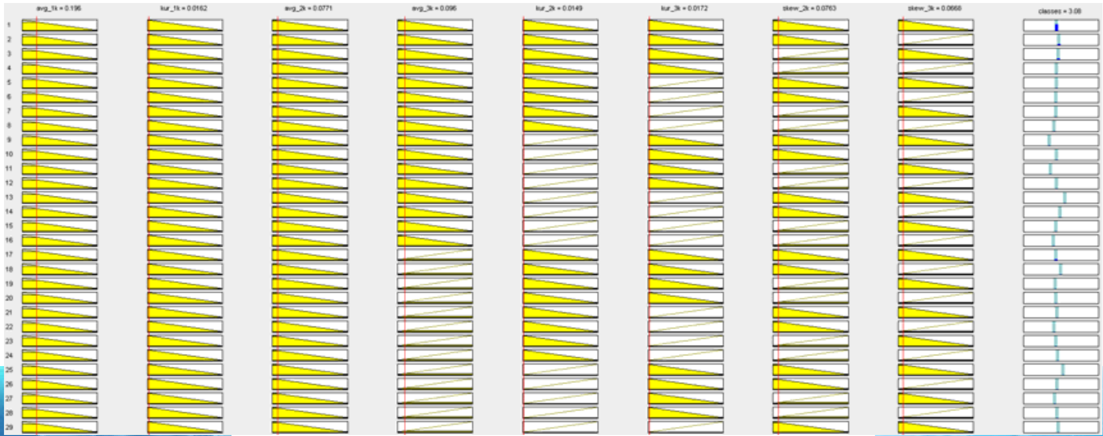

✓ Firing strength of ANFIS rules using chosen data.

Summary of Verification for Explanation of CNNs

- The verification results show that the assumption can now become a correct explanation for CNNs in classifying CWRU bearings.
  - **The features in high-frequency band can be applied for classification more easily for the model instead of focusing at characteristic frequencies which are applied in most researches and traditional diagnosis.**
- The explanation is verified using different techniques to increase the persuasive and correctness of explanation.

ICALAB
智慧型控制及應用實驗室

Verification of Methodology Using Tool Wear Classification (1/2)

- The model is mentioned in applications of CNN with 100% of testing accuracy.
- First, the attention maps of CNN are generated using Grad-CAM.
- The attention map for unworn tools is focusing at frequency bands larger than 5000 Hz while the attention for worn tool is focusing at frequency band lower than 3000 Hz.

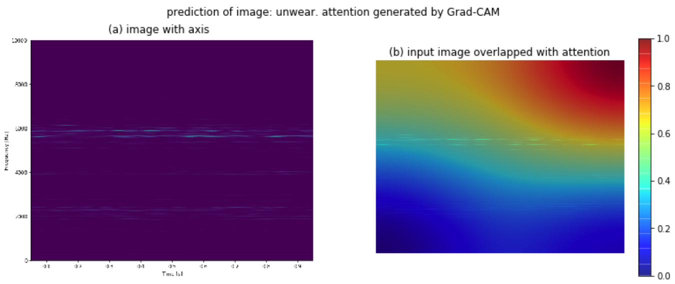

✓ The attention map of model using an unworn tool.

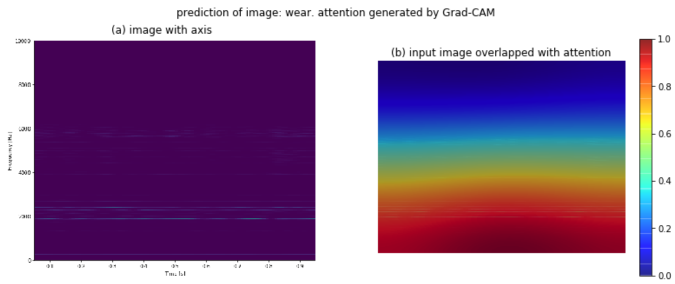

✓ The attention map of model using a worn tool.

Verification of Methodology Using Tool Wear Classification (2/2)

- The features applied for verifications are
  - Average 0~3000 Hz
  - Kurtosis 0~3000 Hz
  - Skewness 0~3000 Hz
  - Average 5001~10000 Hz
  - Kurtosis 5001~10000 Hz
  - Skewness 5001~10000 Hz
- A NN is applied for verification.
- Both training and testing accuracy are 100%.

◆ Structure of NN for classifying tool wear using features in frequency bands with high attention.

Layer	nodes	Activation function
Input layer	6	None
Hidden layer 1	10	Sigmoid
Output layer	2	Softmax

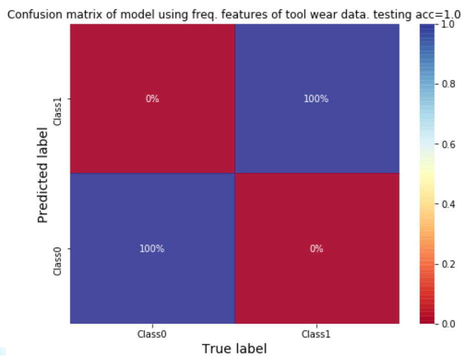

✓ Confusion matrix of NN for classifying tool wear using features focused frequency bands.

Conclusions

- The **interpretability and applications of CNNs** for vibration signals analysis are discussed.
- Applications of CNNs
  - Both 1DCNN and 2DCNN can provide great performances for classification and prediction in vibration signals analysis.
  - By **optimizing** the hyperparameters using **experimental design**, a structure with better performance can be achieved.
- Interpretability of CNNs
  - The **attentions** of models are generated using **Grad-CAM**.
  - By analyzing attentions and verifying, a explanation of classification models of bearing faults can be achieved:
    The features in high-frequency band can be applied for classification more easily for machine learning than **focusing on characteristics computed by traditional signal analysis.**
  - The proposed methodology can be applied in other classification problems of vibration signals analysis.

Other Applications

Tool Wear Estimation System Development & Sensors Selection

Tool Wear Online Monitoring for Quality Control

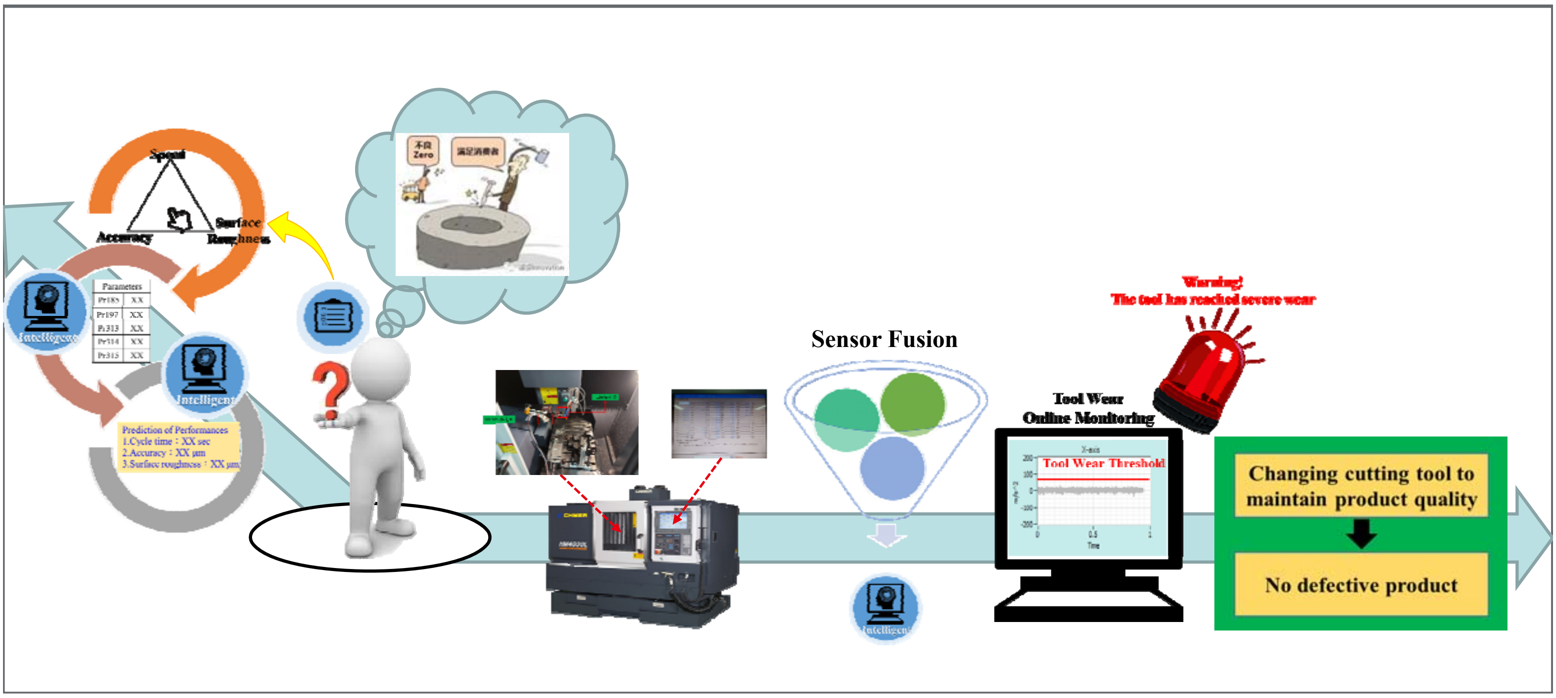

Estimation System Schematic Illustration

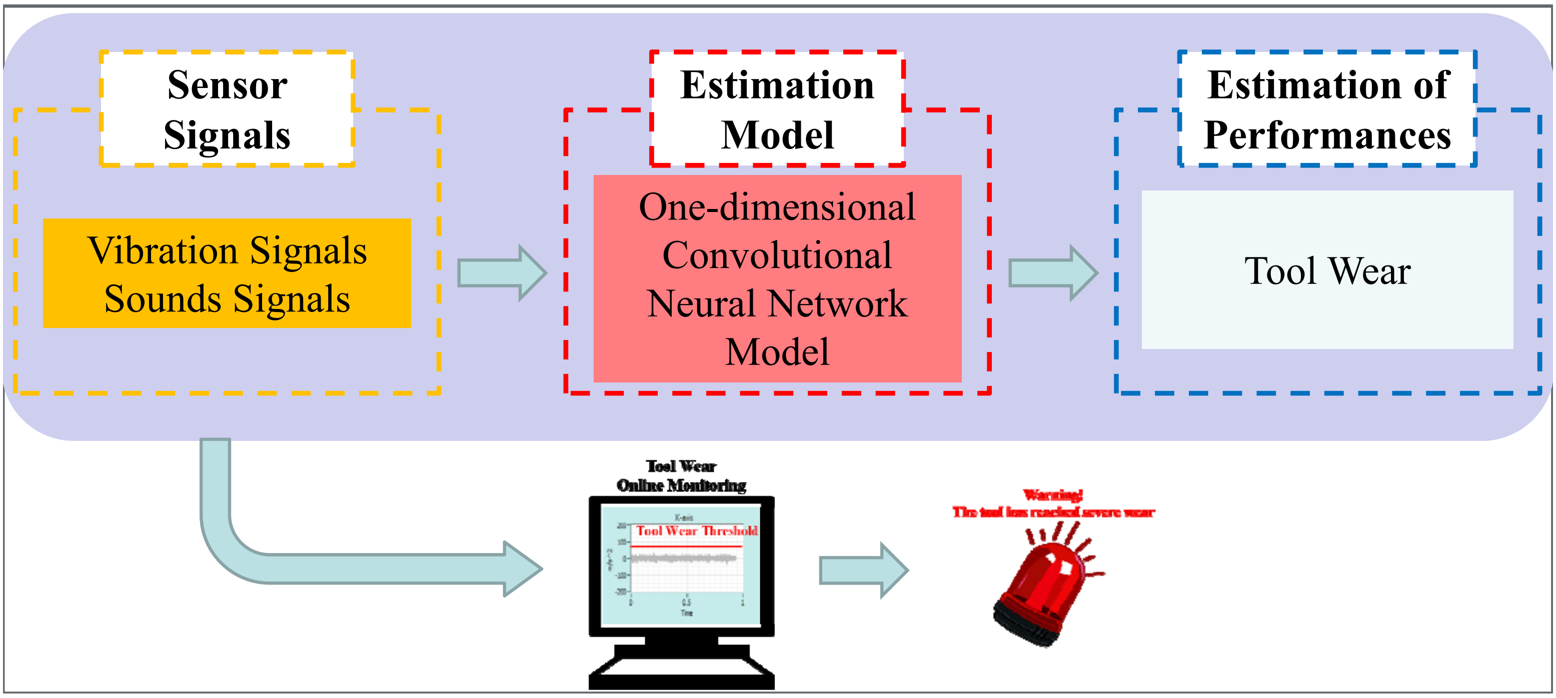

Estimation of Tool Wear – Build Database

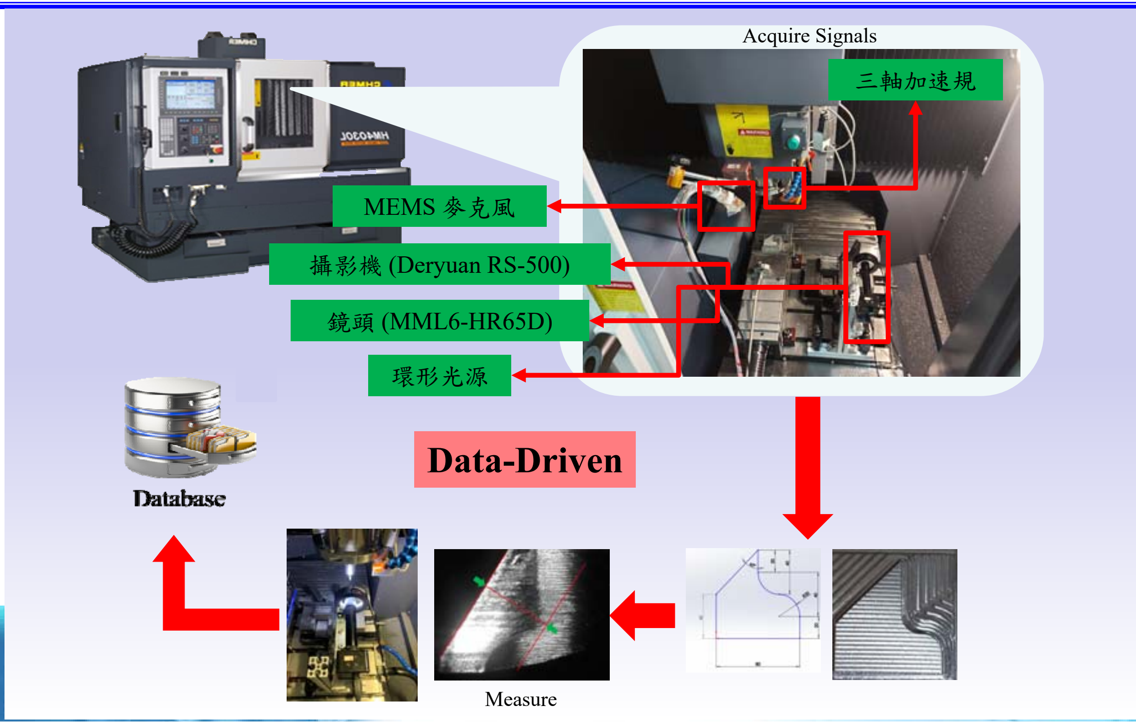

Correlation Analysis

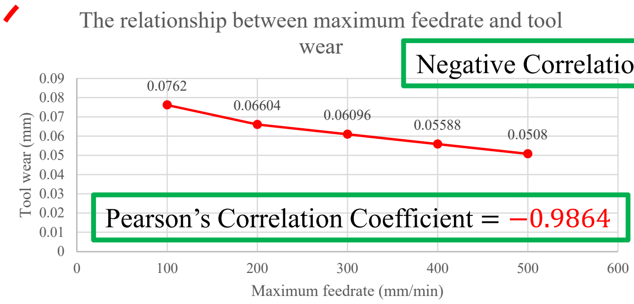

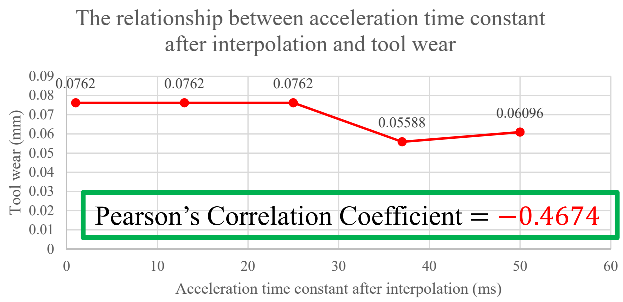

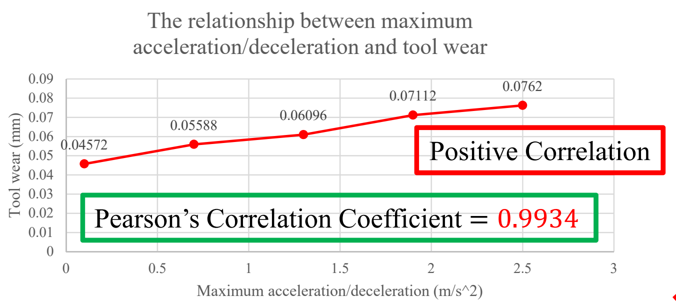

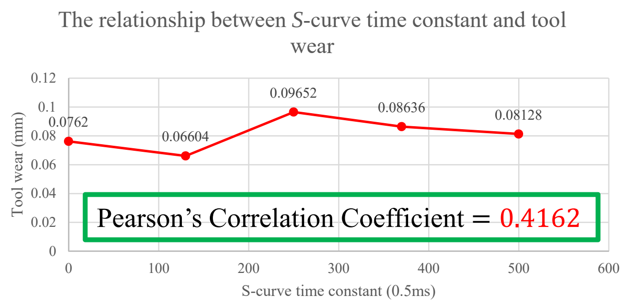

Results of Influential Sensors Selection Analysis

◆ The RMSE values of testing data for tool wear.

Conditions	The RMSE Values of Testing Data					
	X-axial	Y-axial	Z-axial	PCB	MEMS	Current
F120A0.1	0.0494	0.0491	0.0518	0.0452	0.0426	0.0957
F120A1.3	0.0568	0.0615	0.0609	0.0619	0.0684	0.0905
F120A2.5	0.0565	0.0439	0.0453	0.0586	0.0512	0.0906
F240A0.1	0.0583	0.0559	0.0520	0.0768	0.0728	0.0968
F240A1.3	0.0727	0.0705	0.0859	0.0717	0.0836	0.1009
F240A2.5	0.1103	0.0946	0.1077	0.1047	0.1266	0.1199
F360A0.1	0.0980	0.1115	0.1218	0.1381	0.1399	0.1262
F360A1.3	0.0819	0.0795	0.0798	0.0840	0.0872	0.1376
F360A2.5	0.1017	0.0963	0.1021	0.1025	0.1037	0.1359
Average	0.0762	0.0736	0.0786	0.0826	0.0862	0.1105

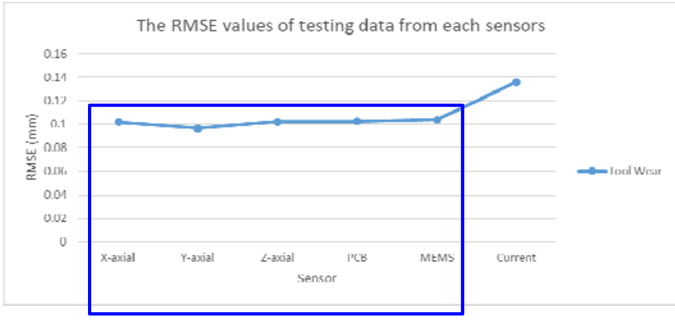

Ranking	Y-axial>X-axial>Z-axial>PCB>MEMS>Current

Estimation of Tool Wear Using 1DCNN Combines with Sensors Fusion

◆ The RMSE values of testing data of the tool wear.

Number	Y-axial	X-axial	Z-axial	PCB	MEMS	Current
1	0.0963	--				
2	0.0612		--			
3	0.0509			--		
4	0.0451				--	
5	**0.0272**					--
6	0.0515					

◆ The RMSE values of testing data of the tool wear for single input.

Conditions	The RMSE Values of Testing Data					
	X-axial	Y-axial	Z-axial	PCB	MEMS	Current
F360A2.5	0.1017	0.0963	0.1021	0.1025	0.1037	0.1359

- **Estimation of Tool Wear Using 1DCNN Combines with Sensors Fusion for Cost Down**

➢ For cost down, MEMS microphone is an industrial technology that combines microelectronics and mechanical engineering, it is cheaper than other sensors which are sound acquirement devices.

➢ According to design of machining path, KAKINO path is a two-dimensional plane (X-Y plane). Therefore, based on cutting theory, the signals of X-axial and Y-axial accelerometers should be considered.

Estimation of Tool Wear - Model Structure

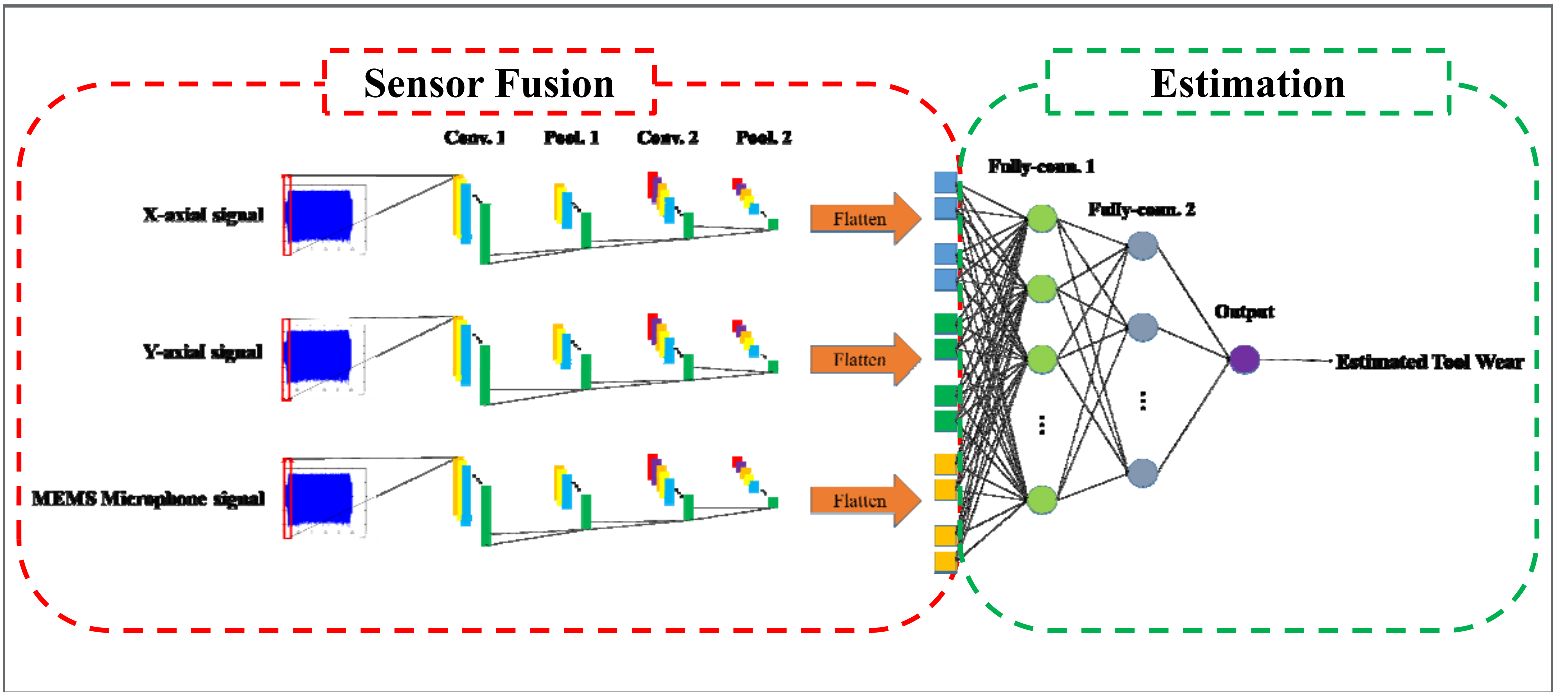

[redacted]

Real-time Tool Wear Detecting Based on a System on Chip

透過單晶片系統取樣加速規訊號 → 資料預處理 → AI 模型計算 → 輸出當前刀具磨耗程度值

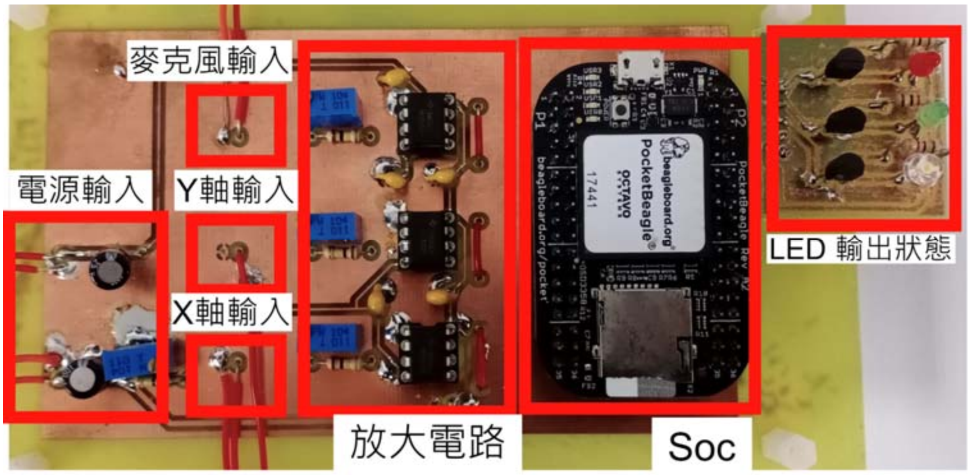

智慧型控制及應用實驗室

Thank you for your attention!

Q&A

ICALAB
智慧型控制及應用實驗室

References

- Han-Yun Chen and Ching-Hung Lee, “Vibration signals analysis by explainable artificial intelligence (XAI) approach: Application on bearing faults,” *IEEE Access* 8, 2020, 134246-134256

- Han-Yun Chen and Ching-Hung Lee, “Deep Learning Approach for Vibration Signals Applications,” *Sensors*, 2021.

- PM Huang, CH Lee, “Estimation of tool wear and surface roughness development using deep learning and sensors fusion,” Sensors 21 (16), 5338

ICALAB
智慧型控制及應用實驗室